

**Loading effects of graphene platelets on  
the microwave absorbing properties of  
co-precipitated nickel ferrite nano  
particles**



**Submitted By**

**Falak Shahzadi**

**School of Chemical and Materials Engineering (SCME)**

**National University of Sciences and Technology**

**(NUST)**

**2017**

**Loading effects of graphene platelets on  
the microwave absorbing properties of  
co-precipitated nickel ferrite nano  
particles.**



**Names: Falak Shahzadi**

**Reg. No:00000118655**

**This thesis is submitted as a partial fulfillment of the requirements for  
the degree of**

**MS in Nanoscience and Engineering**

**Supervisor Name: Dr. Iftikhar Hussain Gul**

**School of Chemical and Materials Engineering (SCME)**

**National University of Sciences and Technology (NUST), H-12  
Islamabad, Pakistan**

**June, 2017**

## **Certificate**

This is to certify that work in this thesis has been carried out by Miss Falak Shahzadi and completed under my supervision in Thermal Transport Laboratory, School of Chemical and Materials Engineering, National University of Sciences and Technology, H-12, Islamabad, Pakistan.

**Supervisor:** \_\_\_\_\_

**Prof. Dr. Iftikhar Hussain Gul**

**Thermal Transport Lab**

**Materials Engineering Department**

**National University of Science and**

**Technology, Islamabad**

Submitted through:

Principal/Dean,

Materials Engineering Department

National University of Sciences and Technology, Islamabad

## **Dedication**

I would like to dedicate this thesis to my family members, my friends and my colleagues for their continuous help and support.

# Acknowledgements

Praise is to the One, the Almighty, the merciful and the beneficent Allah, who is the source of all knowledge and wisdom, taught us what we knew not. We offer our humblest thank to the holy Prophet (Peace be upon him) who is forever a model of guidance and knowledge for humanity.

I am highly indebted to my affectionate supervisor Dr. Iftikhar Hussain Gul for his inspiring guidance, remarkable suggestions, constant encouragement, constructive criticism and co-operation during our project work. Without their support and guidance, this report could not have been possible.

I am also grateful to my family, all my friends and colleagues for giving me encouragement, appreciation and helped in completing this project.

Sincerely,

Falak Shahzadi

# Abstract

The nickel ferrite nano particles were synthesized using co-precipitation method. The composite of nickel ferrite with graphene platelets (0.0%, 5%, 10%, 15%, and 20%) was synthesized by dispersion method. Water was used as a solvent for uniform and homogenous dispersion of nickel ferrite nano particles and graphene platelets. The synthesized sample was characterized using X-ray diffraction (XRD), scanning electron microscopy (SEM) and fourier transform infrared spectroscopy (FTIR). Impedance analyzer and LCR meter was used for performing dielectric measurements and microwave analysis. The formation of single phase face centered cubic  $\text{NiFe}_2\text{O}_4$ /graphene nano composite was confirmed using (XRD). Debye Scherer equation was used to find out the crystallite size that was in range of  $26 \pm 5\text{nm}$ . The attachment of ferrite particles on graphene platelets were observed through (SEM). The band positions were studied using (FTIR). The study of dielectric properties with change in frequency was done at room temperature. The dielectric properties of  $\text{NiFe}_2\text{O}_4$ /graphene platelets showed a huge enhancement leading towards super capacitor behavior of prepared nano composite. For the pure nickel ferrite the real part of dielectric constant was  $1.17 \times 10^4$  and it enhanced to  $3.82 \times 10^{15}$  at 100 Hz for 20% graphene loading. The values of dielectric loss has increased from  $5.15 \times 10^3$  to  $2.96 \times 10^{19}$  at 100 Hz and also the values of tangent loss showed increase from 0.80 to  $7.31 \times 10^5$  at 100 Hz. AC conductivity values also showed increase from  $1.70 \times 10^{-4}$  to  $5.30 \times 10^{11}$  at 100 Hz. AC conductivity results explain that electron hopping governs the conduction process. The decrease in AC impedance is observed with increase in graphene platelet content. The enhanced dielectric properties of the prepared nano composite make it applicable in field of super capacitors. The reflection loss decreases with increase in graphene platelet concentration due to high electrical conductivity of graphene platelets.

# Table of Contents

## Chapter#1: Introduction

1.1	History of ferrites.....	1
1.1.1	Magnetism sources.....	2
1.2	Stratification of magnetic materials.....	2
1.2.1	Para magnetism.....	3
1.2.2	Diamagnetism.....	4
1.2.3	Ferromagnetic and ferromagnetic.....	4
1.2.4	Super-paramagnetism.....	5
1.2.5	Anti-paramagnetism.....	6
1.3	Ferrites.....	6
1.3.1	Hard ferrites.....	6
1.3.2	Soft ferrites.....	7
1.4	Classes of ferrites.....	7
1.4.1	Garnet ferrites.....	7
1.4.2	Spinal ferrites.....	7
1.4.2.1	Types of spinal ferrites.....	8
1.4.3	Hexagonal ferrites.....	9
1.5	Nickel ferrite.....	9
1.6	Significance of ferrites.....	9
1.7	Applications of ferrites.....	10
1.8	Introduction to graphene platelets.....	11
1.9	Objectives.....	12

## Chapter#2: Theoretical Review

2.1	Top down approach.....	13
2.2	Bottom up approach.....	13

2.3	Chemical co-precipitation method.....	21
2.3.1	Prime steps in co-precipitation.....	23
2.3.1.1	Co-precipitation step.....	23
2.3.1.2	Feritisation step.....	23
2.4	Variables include in co-precipitation method...	23
2.4.1	Part of anion.....	24
2.4.1	Speed of blending of reactants.....	24
2.4.3	Impact of pH.....	24
2.4.4	Temperature influence.....	24
2.4.5	Heat treatment after co-precipitation process....	25
2.5	Synthesis of NiFe <sub>2</sub> O <sub>4</sub> .....	25
2.6	Synthesis of NiFe <sub>2</sub> O <sub>4</sub> /graphene platelets comp..	26
2.7	Water as a dispersive medium.....	27

## **Chapter#3: Introduction to characterization techniques**

3.1	X-ray diffraction technique.....	29
3.1.1	Basic principle of XRD.....	30
3.2	Scanning electron microscopy.....	33
3.2.1	Basic principle of SEM.....	34
3.3	Fourier transform infrared spectroscopy.....	34
3.3.1	Working of FTIR.....	35
3.3.2	Applications of FTIR.....	35
3.4	Electrical properties.....	35
3.4.1	Dielectric properties.....	35
3.5	Reflection loss.....	36

## **Chapter#4: Results and discussion**

4.1	X-ray diffraction results.....	37
-----	--------------------------------	----



<b>4.2</b>	<b>SEM results.....</b>	<b>40</b>
<b>4.3</b>	<b>FTIR spectroscopy results.....</b>	<b>43</b>
<b>4.4</b>	<b>Dielectric studies.....</b>	<b>44</b>
<b>4.4.1</b>	<b>Dielectric constant.....</b>	<b>44</b>
<b>4.4.2</b>	<b>Dielectric loss.....</b>	<b>46</b>
<b>4.4.3</b>	<b>Dielectric tangent loss.....</b>	<b>47</b>
<b>4.4.4</b>	<b>Variation of AC conductivity.....</b>	<b>49</b>
<b>4.4.5</b>	<b>AC impedance.....</b>	<b>50</b>
<b>4.5</b>	<b>AC response of materials.....</b>	<b>52</b>
	<b>References.....</b>	<b>56</b>
	<b>Conclusion.....</b>	<b>60</b>
	<b>Future Work.....</b>	<b>61</b>

# List of Figures

## Chapter#1: Introduction

1.1	Configuration of atomic dipoles for paramagnetic materials.....	4
1.2	Atomic dipole ordering for diamagnetic materials.....	4
1.3	Ordering of atomic dipoles for ferromagnetic and ferromagnetic materials.....	5
1.4	Atomic dipole configuration for superparamagnetic materials.....	5
1.5	Ordering of dipoles for antiferromagnetic materials.....	6
1.6	Unit cell of spinal ferrites showing tetrahedral and octahedral sites.....	8

## Chapter#2: Theoretical review

2.1	Steps involved in co-precipitation method.....	22
2.2	Synthesis Process.....	27

## Chapter#3: Introduction to sample characterization techniques

3.1	Incident x-ray beam scattered by atomic plane in a crystal .....	30
3.2	Different cones of radiations forming in powder method.....	31
3.3	Schematic figure of scanning electron microscope.....	34

## Chapter#4: Results and discussion

4.1	XRD pattern of pure graphene platelets.....	37
4.2	XRD patterns of ferrite with increasing graphene concentration..	38
4.3	Crystallite size variation with increasing graphene concentration..	39
4.4	Variation of x-ray and bulk density with graphene weight %.....	39
4.5	Porosity fraction versus graphene weight %.....	40
4.6	SEM image of pure ferrite.....	41

<b>4.7</b>	<b>SEM image of pure graphene platelets.....</b>	<b>41</b>
<b>4.8</b>	<b>SEM image of ferrite with 5% graphene.....</b>	<b>41</b>
<b>4.9</b>	<b>SEM image of ferrite with 10% graphene.....</b>	<b>42</b>
<b>4.10</b>	<b>SEM image of ferrite with 15% graphene.....</b>	<b>42</b>
<b>4.11</b>	<b>SEM image of ferrite with 20% graphene.....</b>	<b>42</b>
<b>4.12</b>	<b>FTIR spectra of prepared ferrites.....</b>	<b>43</b>
<b>4.13</b>	<b>Variation of dielectric constant with frequency.....</b>	<b>45</b>
<b>4.14</b>	<b>Dielectric constant at 100 Hz.....</b>	<b>45</b>
<b>4.15</b>	<b>Variation of dielectric loss with frequency.....</b>	<b>46</b>
<b>4.16</b>	<b>Dielectric loss at 100 Hz.....</b>	<b>47</b>
<b>4.17</b>	<b>Variation of dielectric tangent loss with frequency.....</b>	<b>48</b>
<b>4.18</b>	<b>Dilectric tangent loss at 100 Hz.....</b>	<b>48</b>
<b>4.19</b>	<b>Variation of AC conductivity with frequency.....</b>	<b>49</b>
<b>4.20</b>	<b>AC conductivity at 100 Hz.....</b>	<b>50</b>
<b>4.21</b>	<b>Variation of impedance with frequency.....</b>	<b>51</b>
<b>4.22</b>	<b>Cole-Cole plot of impedance.....</b>	<b>52</b>
<b>4.23(a)</b>	<b>Real Part of permittivity.....</b>	<b>52</b>
<b>4.23(b)</b>	<b>Imaginary Part of permittivity.....</b>	<b>53</b>
<b>4.24</b>	<b>Reflection loss as a function of frequency.....</b>	<b>54</b>

## List of Tables:

### Chapter#4: Results and Discussions

<b>Table No.</b>	<b>Title</b>	<b>Page No.</b>
4.1	Statistics from XRD.....	55
4.2	Statics from dielectric studies.....	55

# Chapter 1

## Introduction

Spinal ferrites have been widely used in electronics applications for last century. It is considered as the most useful ferromagnetic material. They consist of both hard and soft ferrites and they have been in application for past many years. Nano ferrites can be prepared by various methods like hydrothermal, solvothermal, sol-gel, co-precipitation etc. Normally the methods employed can be categorized in two classes' i.e. wet chemical method and solid state method. Usually wet chemical method is preferred because it provides homogenous nano particles also annealing temperature is also low. Wet chemical method usually results in small sized nanoparticles.

### 1.1 History of ferrites

During 470 B.C. specific type of rocks were found in the region near Aegean Sea. These rocks had an ability to attract iron. These rocks were named as Iodestones. The word magnetism was derived from the word magnesia. During 12<sup>th</sup> century Chinese used magnets in navigation tools like compass. During 16<sup>th</sup> century artificial magnets were created by rubbing idoestone with metal pieces. It was also found that the earth has a magnetic field so the compass needle will always point in north-south direction. Charles coulomb and John Michelle made a statement that inverse square law is always obeyed by magnetic poles. In 1825 first electromagnet was prepared. This invention was followed by the fact that electric current can produce magnetic field. Faraday studied all kind of matter including liquids and gases and monitored the impact of magnetism on all of them. Only few of the elements gave a prominent response to the magnetism. Now a days, every kind of machine ranging from simple household machine to heavy industrial machine employ magnets. In order to clearly understand the concept of magnetism the concept of dipole is very important. The variation of energy taking place in a volume space is known as “magnetic field”. This change of energy can easily be calculated and found out. The poles of magnet in a magnetic material can be considered as the entering

and leaving sites for magnetic field. The poles of magnets can never be separated from each other. One magnet has always two poles. These poles exist at the opposite ends in bar magnet. The magnetic field enters the magnet from South Pole and exit the magnet through north pole. A single bar magnet can be made in to two magnets by cutting the single magnet in to two. A magnet can be cut in to half till atomic level. The dipole can be considered as a basic source of magnetism. Magnetism can be considered as the ability of the material to respond a magnetic field. Magnetic field has an attractive effect on some materials and on the other materials it can have repulsive effect. Some materials show no response when magnetic field is applied. Magnetic permeability and magnetic susceptibility relate magnetizing force (H), magnetic flux density (B) and magnetization (M) to each other as shown in following equations.

$$\chi = \frac{\epsilon}{H} \dots\dots\dots(1.1)$$

$$\mu = \frac{B}{H} \dots\dots\dots (1.2)$$

**1.1.1 Magnetism sources**

An atom is the fundamental building block of everything present in this universe. Electron, proton and neutrons are considered as sub atomic elements. Electrons are present outside the nucleus and it revolves around the nucleus. Whereas neutrons and protons exists inside the nucleus. As the electrons are negatively charged so the revolution of electrons around nucleus produces magnetic field. The visualization of subatomic model is hard for mind. Consider an example where a conductor is carrying an electrical current. As the current is motion of electrons, so this movement of electrons creates a magnetic field around conductor. A compass needle can be used for the detection of this magnetic field. This needle will behave like a dipole due to the force acting upon it. All the existing materials respond to magnetic field in a unique way.

**1.2 Stratification of magnetic materials**

The placement of material in a magnetic field makes it respond differently to the field. This difference in behavior can be attributed to many factors like atomic or

molecular structure or collective magnetic moment of the entire atom. The spin and orbital motion of electrons considerably affect the magnetic moment. Also the spin and orbital motion is changed by magnetic field applied externally. The applied magnetic field made some materials to align parallel while some materials align opposite to applied electric field. The atoms consisting of paired electrons, magnetic field got cancelled due to their spinning in the opposite direction. As a result of opposite spinning the electrons cancel the magnetic field produced by each other. While the atoms are having unpaired number of electrons has some value of net magnetic field. These characteristics dictate the behavior of material in response to magnetic field [1]. The magnetic behaviors can be categorized as follows:

1. Para magnetism
2. Diamagnetism
3. Ferro/Ferrimagnetism
4. Super-Para magnetism
5. Antiferromagnetism

### **1.2.1 Para magnetism**

The Para magnetism arises when the orbital and spin magnetic moment does not completely cancel with each other. This will create permanent dipole moments and this will result in Para magnetism. In the absence of any magnetic field the dipoles are randomly oriented in domains. This will result in zero net magnetization. The net magnetization is acquired by applying magnetic field. The magnetic field will align the magnetic moments in direction of field and this will result in some net magnetization [2].

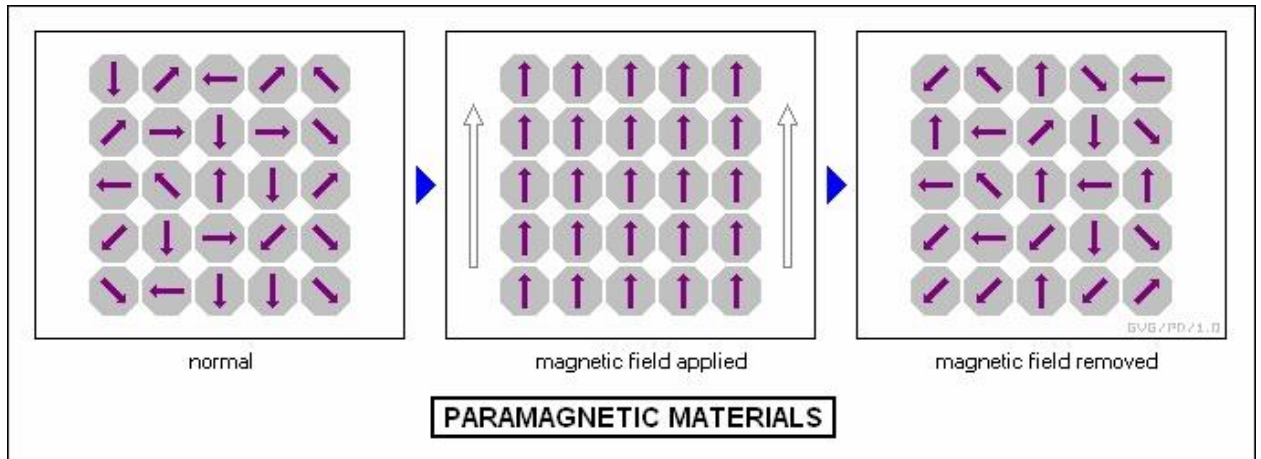


**Fig 1.1 Configuration of atomic dipoles for a paramagnetic material [3]**

### 1.2.2 Diamagnetism

The electron's orbital motion in presence of magnetic field will give rise to diamagnetism. The diamagnetism exists when the net magnetic moment of atom is zero. The atom's orbital motion produces a magnetic field that opposes the applied magnetic field. This is explained by negative susceptibility. The movement of material is towards the place where the strength of magnetic field is weak.

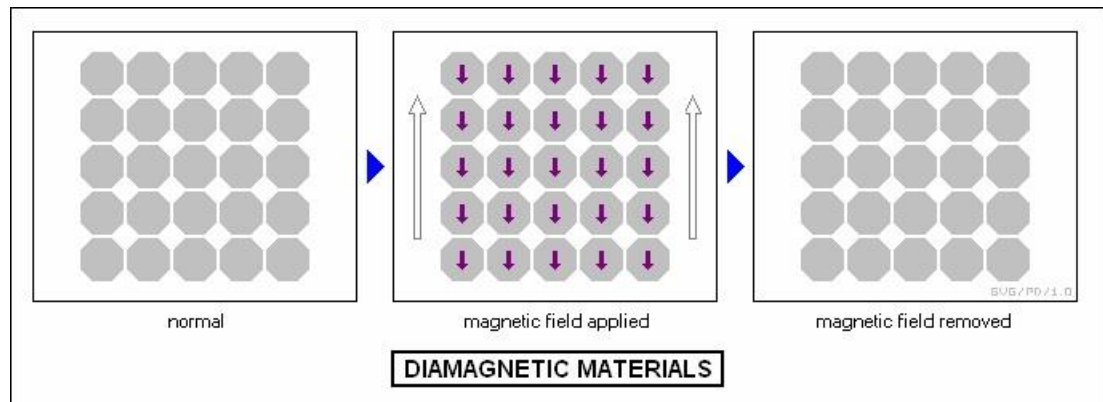


**Fig 1.2 Atomic dipole ordering for a diamagnetic material [3]**

### 1.2.3 Ferromagnetism and ferrimagnetism

The material which possess permanent magnetization in the absence of external magnetic field are known as ferromagnetic and ferri magnetic materials. Permanent magnetization value is large in these materials. Atoms spins, also known as domains,



interact with each other in such a way that will result in the alignment of all spins in same direction [4].

The permanent magnetization observed in case of ferromagnetic materials is due to incomplete magnetic field cancellation. This will result in a magnetization which is permanent but of low magnitude. If all the domains present in the sample get aligned then their sum will result in macroscopic magnetization in ferromagnetic and ferromagnetic materials. Ionic solids are electrically insulating so is ferromagnetic materials. Ferromagnetic materials are mostly metals.

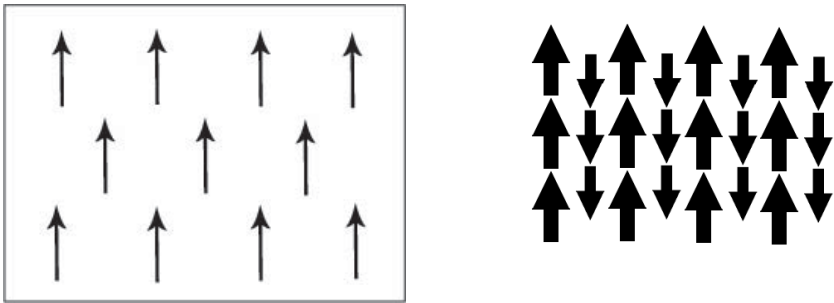


**Fig 1.3 Ordering of dipoles for ferromagnetic and ferrimagnetic behavior [3]**

**1.2.4 Super-para magnetism**

The super Para magnetism arises when a material is subjected to temperature less than curie temperature. This will result in the alignment of neighboring atom’s magnetic moments [5].

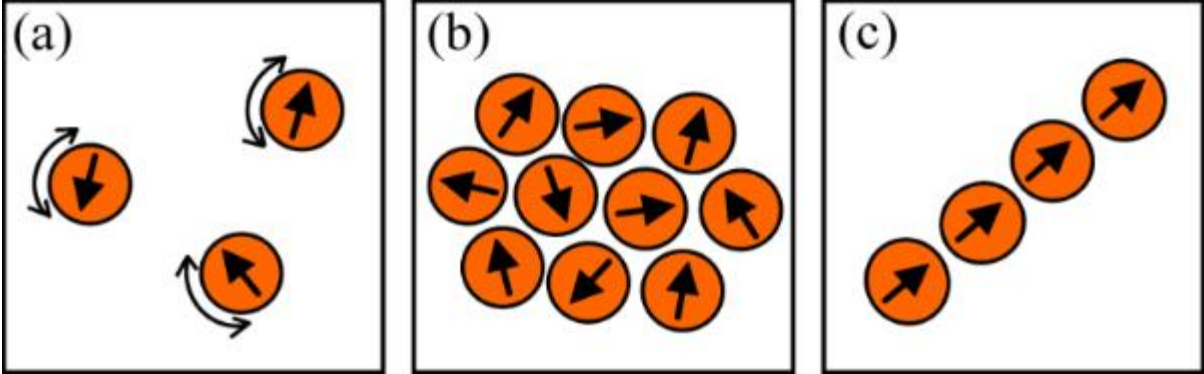


**Fig 1.4 Atomic dipole configuration for super-paramagnetic behavior [6]**

### 1.2.5 Anti-ferromagnetism

The magnetic moments or electron spins aligned in regular pattern to the spins of neighboring atoms but oriented in opposite direction will result in anti-ferromagnetism. This specific kind of behavior is observed at very low temperature and it vanishes above a fixed temperature. This temperature is known as Neel temperature [7].

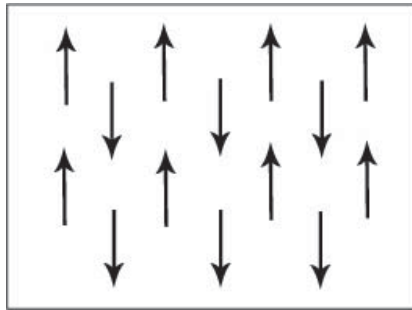


**Fig 1.5 Ordering of dipoles for anti-ferromagnetism [6]**

## 1.3 Ferrites

The ferromagnetic materials consist of ferrites as one of their important elements. The main component of ferrite is oxide of iron. The existence of ferromagnetic oxides makes ferrites insulating in nature. Due to the magnetic nature of ferrites, they are used in many applications including permanent magnets and transformer cores. The unique ability to hinder the production of eddy currents due to their highly resistive nature makes them useful in applications involving high frequencies. Ferrites have a high electrical resistivity values. On the bases of hysteresis losses the ferrites are divided in to two types i.e. hexagonal structure and cubic structure. The mass and charge of metallic ions forms the bases of these symmetries.

### 1.3.1 Hard ferrites

Another name for hard ferrites is ceramic magnets. They are highly coercive in nature so the time taken by them to demagnetize is large. Hard ferrites have high value of magnetic permeability. Oxides of barium, iron and strontium contribute in making hard ferrites. The material required for synthesis of hard ferrites is easily available so

they are less expensive. Their low cost make them applicable in household items [1]. Ferrites of cobalt and strontium are the example of hard ferrites.

### **1.3.2 Soft ferrites**

The soft ferrites have low values of coercivity. They also show low energy dissipation value during magnetization. Their appearance is usually dark in color e.g. gray or black. Soft ferrites are usually brittle and hard. The value of resistivity is also high. They are applicable in inductors and transformer cores so that energy losses can be minimized. Some examples of soft ferrites include zinc and nickel ferrite [1].

## **1.4 Classes of ferrites**

On the basis of structure the ferrites are divided in to three types which are as follows:

- Garnet ferrites
- Spinal ferrites
- Hexagonal ferrites

### **1.4.1 Garnet ferrites**

The Garnets were discovered in 1957 by Galileo. The general formula for garnets is  $M_3Fe_5O_{12}$  and they occupy a cubic structure. Where M represents trivalent ion of rare earth metal. Some of the examples of trivalent ions of rare earth metals are Y, Dy, Gd etc. Garnets generally fall in the category of hard materials.

### **1.4.2 Spinal ferrites**

The general formula for spinel ferrites is  $MFe_2O_4$ . Where M represent divalent cations. The example of divalent cations include nickel ( $Ni^{+2}$ ), copper ( $Cu^{+2}$ ), zinc ( $Zn^{+2}$ ), cobalt ( $Co^{+2}$ ) etc. Among all the types of ferrite, spinal ferrites have comparatively simple structure. The number of oxygen ions present in its unit cell is 32. The arrangement of anions obeys face centered cubic closed packed structure. The two types of sites A and B present between anions are referred as tetrahedral and octahedral sites respectively. The number of oxygen atom surrounding a tetrahedral site is 4. There

are 64 tetrahedral sites in a spinel structure. The cations are present on 8 tetrahedral sites. The number of oxygen atoms surrounding an octahedral site is 6. The number of octahedral sites present in a spinel structure is 32. The anions are present on 16 octahedral sites. The spinel structure is electrically neutral due to presence of A and B sites.

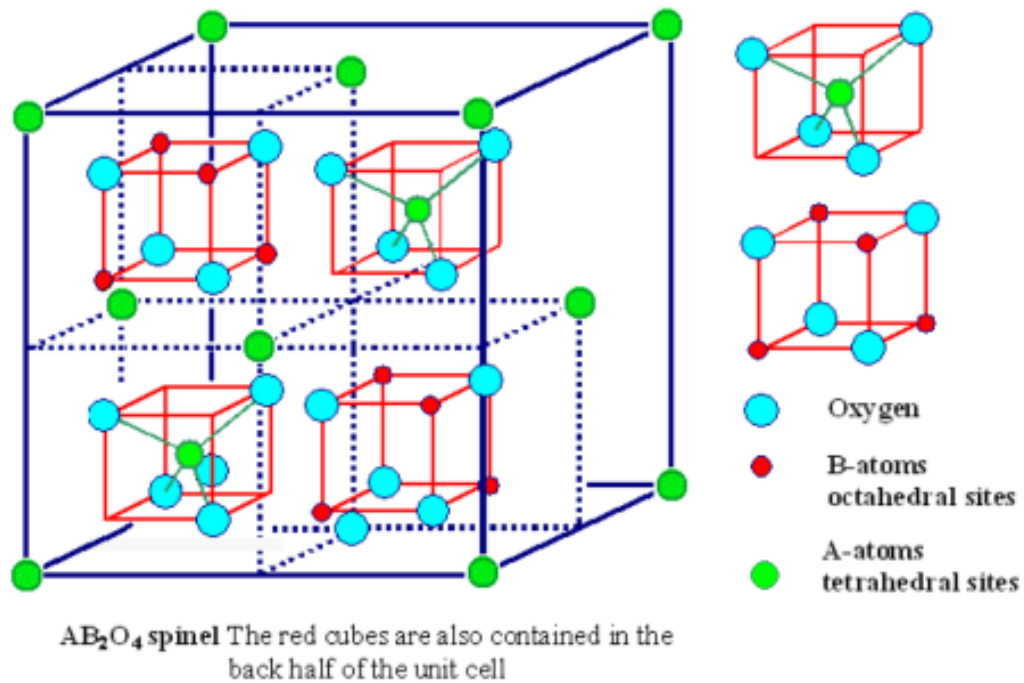


**Fig 1.6 Unit cell of spinel ferrites showing tetrahedral and octahedral sites [1]**

### 1.3.2.1 Types of spinel ferrites

There are two types of spinel structure namely:

- (a) Inverse spinel
- (b) Normal spinel

In a crystal lattice, the trivalent ions present in inverse spinel ferrites are present on both A and B sites whereas the divalent ions are present on B sites.

In a crystal lattice, the divalent metal ions are present on A site and trivalent metal ions occupy B sites in the normal ferrites.

### **1.4.3 Hexagonal ferrites**

The hexagonal ferrites obey the formula  $MFe_{12}O_{19}$ . Where M represent barium, cobalt, strontium etc. or their combination. The coercivity value of hexagonal ferrites is very high so they are applicable as permanent magnets. The crystal structure resembles hexagonal structure. Three sites are occupied by metal ions. These sites are tetrahedral, octahedral and trigonal. The applications of magnetic materials include loud speakers, recording devices, microwave applications and much more.

## **1.4 Nickel ferrite**

Since 1940s, nickel ferrite has considered to be a vital material for its application in microwave devices. It is useful because its microwave loss is very low. It has a high Neel temperature. It also has low values of magnetostriction and magnetic anisotropy. The electronic structure of nickel ferrite resembles to Mott insulator. There is a strong repulsive forces present between d electrons. As a result of these repulsive forces the d band, which is partially filled, splits up in to lower and upper Hubbard bands. This repulsion will result in the formation of local magnetic moments and electronic ground state. Neel configuration helped in order to make better understanding of magnetic structure of nickel ferrite. The nearest neighboring sites have strong and dominant antiferromagnetic interaction. Oxygen serves as a carrier in this interaction. As a result the magnetic moments of sites A and B align anti-parallel to each other.

Increase in AC conductivity is observed as the frequency increases. The impurities and defects will result in dielectric loss. The increase in frequency will also cause dielectric constant to increase. At frequencies above 10 KHz the value of dielectric constant decreases. As the frequency increases the ferrites convert from ferromagnetic to paramagnetic so this will result in decrease in value of dielectric constant. The variations in temperature also effect the value of dielectric constant.

## **1.5 Significance of ferrites**

The magnetic materials like iron and its alloys are used in various technologies. The reason for their use is their low DC resistivity. But some applications like electrical

circuits and cores of inductors cannot make use of iron and its alloys as these are applications requiring high frequencies. The current that induce in the circuit start flowing in the material. This problem is heat generation due to presence of low electrical resistivity. This will result in the release of energy in atmosphere posing serious issues. The energy losses make the material incompatible at high frequencies. The ferrites, on the other hand, showed better performance because of their high DC resistivity values. Some properties like relatively high permeability and stability with temperature have also opened way for its use in applications involving high frequencies like electronic circuits, adjustable inductors, filter circuits and delay lines etc. The ferrite applications for high frequencies are more usual. Another reason for their use is they are relatively less expensive compared to other alloys. In case of material requirement that has low volume, high quality, low cost and high stability, ferrites are considered to be best for frequency ranges of 10 KHz to Mhz. Also ferrites offer flexible mechanical and magnetic parameter that none of other metal has offered.

## **1.6 Application of ferrites**

As ferrites have a high value of electrical resistivity so they are considered to be very useful nano particles. Ferrites have many applications especially at high frequencies [8]. Following properties enable the wide use of ferrites:

- They are less expensive.
- Some ferrites have high values of coactivity.
- They are mechanically stiff.
- They offer time and temperature stability.
- They are applicable at microwave frequencies.
- They are used in applications involving high frequencies.
- They offer selection of material over wide range.

The DC resistivity of ferrite nano particles is significantly high. They offer good magnetic properties and are chemically stable at high temperatures. The eddy current loss value is also very low. These properties make ferrite applicable in following application:

- Application in electromagnetic absorbers.
- Application in drug delivery.
- Application as Ferro fluids.
- Application as data storage materials.
- Application in microwave devices.

## **1.8 Introduction to graphene platelets**

Graphene is a two dimensional allotropic form of carbon. It is a hexagon with one atom present at each corner. Graphene can be seen as a large aromatic molecule. It is a two dimensional structure where bonds are present between atoms. These bonds hold the structure together. The hexagonal rings are present in every layer of graphene. As a result it appears as a honey comb structure. Usually the thickness of layer is one atom. Three million layers need to be put together in order to make graphene sheet of thickness 1mm.

Graphene has an ordered structure because there is tight bonding present between atoms. As carbon is non-metal but graphene behave as a metal or semi metal as its conductivity lies between conductor and insulator. Graphene is one of the strongest materials discovered until now. Graphene shows both the stiffness and elastic properties. It can be stretched without breakage. The flat planes present in it can easily reflex without allowing atoms to break apart. Also it is a light weight material. As the layer of graphene is only one atom thick so it is very light weight material. It has high values of thermal conductivity. They can be used to ass heat resistance or conductivity to some materials like plastics etc. Their thermal conductivity is better than silver and copper.

The electrical conductivity of graphene is also high. Very less resistance is offered to electrons by hexagonal structure of graphene. This will result in fast conductivity like conductors or super conductors. The mean free path of electrons is very high. The use of graphene can revolutionize electricity production. The electrons are mobile in graphene this will make it applicable in computer chips. As layers of graphene are thin so they are transparent. It transmits most of the light that falls on it. This property can be applicable in solar cells. Gas trapping and detection can be done by

making traps of graphene. It can also serve as a material for holding gases. It can store hydrogen and make fuel cars running utilizing hydrogen possible.

As compared to other nano materials nano graphene platelets have shown remarkable characteristics. They are applicable in following industries:

- Automotive
- Energy
- Aerospace
- Marine
- Electronics
- Medical
- Construction
- Telecommunication

## **1.9 Objectives**

The objectives of this research work are as follows:

- Using a simple and inexpensive chemical co-precipitation method for synthesis of  $\text{NiFe}_2\text{O}_4$  nanoparticles having single phase and spinal structure.
- Using water as a dispersive medium for synthesis of  $\text{NiFe}_2\text{O}_4$  /graphene platelets nano composite.
- Study the effect of graphene platelets loadings on microwave properties of  $\text{NiFe}_2\text{O}_4$  nanoparticles and their composite with graphene platelets.



# Chapter 2

## Theoretical Review

Nanoparticles can be synthesized by following two ways:

- Top down approach
- Bottom up approach

### 2.1 Top down approach

Top down approach involves the cutting of bulk material into nano sized particles. A large amount of useful nanostructures are fabricated by using various top-down fabrication techniques. Some of these techniques are molding, lithography, embossing and skiving [9]. In lithography, electron or light beam is made to fall on a selective portion of device. A variety of elements in semiconductor industry is made using lithography. For instance integrated circuits, masks etc. ceramic industry also employ top down method for making alloys.

Top-down method has variety of applications on commercial level. Also there are some drawbacks associated with top-down method.

- A significant amount of impurity is present in the products synthesized using this method.
- The structure established initially might have to be changed in roll-out phase.

### 2.2 Bottom up approach

In bottom-up approach, atoms and molecules combine together to form complex and stable structures. This is most widely used technique for synthesis of nano particles. Bottom-up technique includes chemical vapor deposition, molecular beam epitaxy, physical vapor deposition, electrochemical deposition, sol-gel, co-precipitation methods etc. It offers various advantages i.e. it is better, cheaper, easy to handle and efficient.

Nanoparticles can be synthesized by various methods. Every method poses a separate advantages and disadvantages. The chemical, structural and magnetic properties of synthesized nano particles depend greatly on the method used for synthesis. Some of the synthesis methods are as follows.

- Sol-gel method.
- Micro emulsion method.
- Co-precipitation method.
- Solvothermal method.
- Hydrothermal method.
- Gas condensation method.
- Sono-chemical method.
- Combustion flame synthesis.

At room temperature ferrites exhibit unique behavior and are applicable to many devices due to their unique properties. Ferrites have low electrical losses and high DC electrical resistivity. Spinal ferrites are preferred due to chemical stability, excellent magnetic properties, simplified synthesis process, reasonable cost and mechanical hardness [10, 11]. Presently ferrites are applicable in antennas cores, computer components, memory devices, permanent magnets, satellite communication, magnetic sensors and actuators, microwave absorbing materials, gas sensors, cancer treatment and in magnetic resonance imaging [12]. Due to fine electrochemical performance, binary metal oxides are extensively applicable in electrochemical applications, like capacitors [13], fuel cells [14], Li-ion batteries [15], solar cells [16]. Electrochemical capacitors employ oxides of transition metals having a spinal crystal structure, as they provide a strong crystalline architecture with diffusion pathways in three dimensions [17]. Presently a variety of spinal and inverse spinal ferrites have been tested for electrochemical capacitors. Electronics and catalysis have been extensively employed transition metal oxides because of their high catalytic activity, environmental accordance and easy separation [18, 19]. Graphene is an interesting carbon nanomaterial having two dimensions. Due to its remarkable electrical conductivity, ultrathin nanostructure and mechanical stability, graphene is broadly used as an electrode material for super

capacitors [20-22]. Recently published research work showed applicability of transition metal oxide/graphene composite as electrochemical materials [23-25]. Transition metal oxides work together with graphene to enhance electrochemical performance of hybrid material. In these hybrids, graphene work as a conductive backbone in order to make electron transfer smother. Graphene also serve as a mechanical structure that prolongs the uprightness of electrode throughout the electrochemical process [26]. Moreover composite of metal oxide with graphene is cost effective and optimistic method to gain high super capacitor performance [27].

In this study, nickel ferrite/graphene (Graphene=0.0%, 5%, 10%, 15% and 20%) nano composite is prepared for investigation of microstructural, structural, dielectric properties and AC conductivity at different frequency range. Various chemical routes can be used for the synthesis of nickel ferrite nanoparticles i.e. hydrothermal [28], co-precipitation [29], sol-gel [30], solvothermal [31], micro emulsion [32] and other methods. Nickel ferrite nanoparticles were prepared by wet chemical co-precipitation method in present study. This method is used because it is cheap, quick, easily controllable and low calcination temperature [33]. The particle size and properties depends on various conditions like pH, temperature, stirring rate etc. The ultrasonic method was used for the synthesis of nickel ferrite/graphene nano composite. Deionized water was used as a dispersion medium for the dispersion of graphene platelets and nickel ferrite nanoparticles. The generation of spinal phase ferrite and presence of graphene was studied using XRD and SEM. The presence of functional groups was investigated using FTIR. The dielectric properties as a function of frequency were also studied using two probe method at room temperature.

After the year 2000, the magnitude of work related to synthesis and characterization of ferrite nanoparticles have gain popularity. The change in property of material at Nano scale was the main cause for this increased research work. The main focus of many conferences was to develop processing equipment and development of characterization techniques for synthesis and characterization of ferrites. Also the application of ferrite particle in optical applications, microwave applications, multilayer chips inductor and

nano ferrite composite were considered. Dr. J.L. Snock concept about ferrite was used by Japanese scientist [34].

**H.S. Singh et al.** worked on ferrite nanoparticles due to their remarkable dielectric and electric properties. They worked on nickel ferrite and substituted nickel ferrite. The magnetic, electric and physical properties of nickel showed a remarkable improve when it is substituted with Aluminum. So it can be concluded that the properties can be enhanced by making composite of nickel with other material. The study is needed to know the exact amount of substitution and method of preparation. The effect of preparation technique should also be known [35].

**Roul Valenzuda** studied the application of ferrites in different fields. He also studied the composite of ferrites with other material. The electromagnetic interference arises due to considerable increase in usage of electronic equipment. The presence of high speed digital interfaces in computers, sensors are passing huge rest of disturbance caused by them. The electric and magnetic field also causes interference in wireless system. The electromagnetic system causes disturbance in working of electronic system. This is considered an electromagnetic interference. The electrical devices usually produce noise at frequency mostly larger compared to signals of circuit. In order to reduce the interference, the particles designed should behave similar to low power filters. This will enable the circuit to not reject the frequencies higher than given value of frequency [36].

**A.E. Paladino et al.** studied microwave properties of fine grain nickel ferrite at high peak power levels. The process used for synthesis of ferrite nanoparticles was hot press ball milling and composite is prepared using flame spraying. The studies find out that with decrease in grain size absorption is increased. The value of dielectric loss also shows a reduction. The dielectric losses offered by low field also reduces with composition. Cobalt is also substituted in higher threshold fields. The prepared fine grained ferrite which was also hot pressed has operated at 750 KW/750 W power level. But a nonlinear behavior was observed below peak power of 20 kW [37].

**A.P. Singh et al.** studied the microwave properties of conducting magnetic Nano composites. They suggested that the electromagnetic properties of a composite having

multiple phases can be improved by various methods. These methods include introduction of magnetic filler in a reasonable amount. Other method involves the design of such a medium that contain conducting magnetic and dielectric material mixture as filler. A lot of studies have done in this field but scientists are still unable to find out a material that will produce no reflection and give competent absorption. This is a challenging task the only possible solution is the use of materials which can also be seen as the future possibility. The next generation material will form the building blocks of shielding material will be multi-phase and light weight materials having excellent shielding properties [38].

**D.I. Zoha et al.** synthesized composite of nickel ferrite with graphene and studied their photo catalytic properties. The method used for synthesis was by using polyacrylamide gel and the size of the prepared particles of ferrite was 31nm. The composite of ferrite and graphene was prepared by sol gel chemical method by dispersing ferrite and graphene in ethanol and drying afterwards. The results showed excellent adhesion of ferrite particles in graphene sheets. Methylene blue was used to find out photo catalytic activity of sample. The degradation was performed under stimulated sunlight. The results showed enhanced and improved photocatalytic performance in comparison to simple nickel ferrite. The presence of hydroxyl radical was confirmed by using photoluminescence. They were found to be irradiated on nickel ferrite graphene composite. The specie that plays an active role in degradation is hydroxyl radical [24].

Various methods have been used to prepare an EMI suppression like by using ferromagnetic materials and their composites, soft ferrites, carbon nanotube material etc. **R.C. Chie at al.** combines carbon nanomaterial with ferrite. The resulting composite showed excellent microwave absorbing properties. The composite of carbon nanotube/cobalt ferrite was prepared by chemical vapor deposition in which cobalt ferrite work as catalyst. The results showed enhanced microwave absorption. The electromagnetic waves energy loss comes from dielectric loss of carbon nanotube. In case of ferrite magnetic loss contribute to the increase of microwave absorption. In isolation both are not good absorbers. In case of nano composite there is a good plot of

magnetic loss and dielectric loss. This happens due to combining ferroelectric material and paramagnetic nanotubes. This will result in improved microwave absorption. The cobalt ferrite nanoparticles, which are dispersed, use resonance phenomena to absorb signal. Their shape and nature of interaction enable them to do so. In case of congregated particles all these interactions are not significant [39].

**Zehra et al.** worked on graphene and its composite with hard ferrite to find out microwave absorbing properties. Barium ferrite nanoparticles were prepared by using sol gel method. They are combining with graphene sheets. The barium hexa ferrite nanoparticles were made to deposit on graphene sheets which are of thickness nanometer. The novel composite as prepared to check its microwave absorbing properties. The barium ferrite nanoparticles embedded on graphene has increased absorption. Due to layered structure the shielding activity shows much better results. The mechanism involves multiple reflections. Absorption is reason for enhance performance. The physical and structural properties show graphene/ barium ferrite to have enhanced microwave absorbing properties [40].

**Zhao et al.** studied the dielectric and microwave properties of graphene nano platelets and epoxy composites. Graphene Nano platelets were prepared by plasma exfoliation process. The sono chemical method was used for preparation of composite. The resulting composite showed enhanced dielectric permittivity, reflection loss and conductivity. The graphene nano platelets interact with microwave radiations resulting in attenuation of electromagnetic energy. This will enhance microwave absorbance properties. The increase in conductivity will decrease in dielectric loss. The polarization at interface cause this phenomena, also there is an impedance mismatch that will cause decrease in reflection loss. The higher loadings of graphene nano platelets will result in less reflection loss and impedance mismatch that occur at interface of composite and air. High quality electromagnetic wave absorbing devices can be prepared using this composite as it shows high reflection loss that can be tuned [41].

**Shahid Ameer et al.** studied the effects of reduced graphene oxide on absorption band with the nano composite of nickel ferrite and reduced graphene oxide by solvo thermal methods. The graphene sheets used had large diameter. The solvo thermal

method served for two purposes i.e. in composite formation and in reduction. In order to obtain high microwave absorption properties, the properties were tailored. Thus, the resulting nano composite showed excellent microwave absorbing properties [42].

**Lili Zhang et al.** synthesized iron oxide composite with reduced graphene oxide and tested it for microwave absorption at high temperature. The composite was prepared using facile thermo-chemical reactions. Due to electromagnetic effect the prepared sample showed enhanced electromagnetic absorbance. The composite prepared by this method has shown better results in comparison to other methods. This shows the importance of synthesized methods, these samples are stable and show excellent absorbance at high temperature even better than commercially available absorbers [43].

**Christopher R. Herron** used scalable and simple method to synthesize thin films of grapheme and also few layer grapheme platelets using bottom up synthesis approach. Andy Wieto et al. used spark plasma sintering for synthesis of graphene nano platelets and then studied their properties. The spark plasma synthesis method was used in order to synthesize graphene nano platelets bulk sample. The pressure during the process was 80MPa and temperature of 1850 degree Celsius was maintained. Graphene nano platelets have ability to maintain their structure and they are able to bear extreme sintering conditions. The structure of graphene nano platelets allow it to stay unbreakable during spark plasma synthesis process while carbon nano tubes break during this process. The structure of graphene nano platelets are two dimensional. The structure of nano tubes is in tubular form so it can collapse easily when subjected to high pressure. The synthesis of graphene nano platelets in bulk enable to study various phenomena's and mechanisms directly. Knowledge of these phenomena's and mechanisms help to access the behavior of graphene nano platelets in composites where they behave as secondary phase. The structure of resultant graphene nano platelets was corrugated. This will help in dissipation of energy when load is applied on material. Graphene nano platelets are considered as great reinforcing agent in ceramics due to their unique blending mechanism. The toughness of the composite has also increased because graphene nano platelets stop the propagation of cracks and defects. Graphene nano platelets work as; lubricants and in presence of high loading it shear off. So it can

be concluded that synthesized graphene nano platelets increased toughness and reduced friction [44].

**Xiqing yuan et al.** has done facile synthesis of graphene platelets that are mesoporous in nature and utilized them for lithium ion batteries. The graphene platelets were doped with sulfur and nitrogen. The doping is carried out by novel method. L-cysteine is used as a carbon precursor on a water soluble salt. This water soluble salt act as a template. There are nitrogen, sulfur and ammine group present in L-cystine. These groups can be functionalized by carboxylic group. There is abundance of sulfur and nitrogen sites and it is considered to exhibit good conductivity. The composite capability to be used as cathode material was measured. The preparation involves sodium chloride as a template salt. It also plays an important role in forming structure. Also the non-toxicity and easy availability serves important purpose. A lot of active sites are present which are homogenous in nature. The mesoporous structure was formed that contain sulfur as host atom. It also provides pores for lithium ion batteries. The capacity of discharge was also increase due to presence of lithium polysulfide. The composite of graphene nanoplatelets and sulfur has high current density also the discharge capacity is enhanced. This process will enable the novel design of cathode material for production of Li-S batteries [45].

**Dinesh kumar et al.** synthesized graphene nano platelets using microwave assisted method. Rapid microwave exfoliation was used for synthesis of graphene nano platelets. The process also involved expandable graphite. The microwaves were made to fall on expandable graphite for three minutes. Later on sulphuric and nitric acid were used for the completion of process. The graphene nano platelets prepared by this method were analyzed using different characterization techniques. The graphene nano platelets prepared by this method has very high purity. There was no serious structural damage that cannot be recovered. The traces of oxides were also available. The synthesized graphene nano platelets were little thick in layer, variable in size and considerably crystalline. The microwave method for producing graphene sheets is an effective and versatile method. It has various advantages like energy transfer occur in place of heat



transfer. It is ecofriendly and safe. The rate of reaction is also several orders of magnitude faster. It also involves volumetric heating which is quick and fast [46].

**Y.C yang et al.** studied nickel ferrite and its electrical, magnetic and structural properties. Also composite of nickel ferrite with transition metals and rare earth metal was studied. The particles were prepared by different routes including sol-gel method and co precipitation method and a comparison is made between them. The particles prepared by sol-gel method were big in size, highly resistive, ferromagnetic and multi-domain. The prepared particles can be used in applications involving high frequency. The particles prepared by co precipitation method were smaller in size, paramagnetic and had single domain. The prepared particles are applicable in magnetic resonance imaging, drug delivery, medical applications etc. when nickel ferrite is doped with rare earth element the reduction in magnetization is observed. The increase in coercivity is observed by adding transition metal. The decrease in dielectric loss is observed when doped with rare earth metal ions. Particle size increase in case of doping with transition elements. The lattice constant is also observed to increase with doping. The unit cell is also observed to expand. Further studies suggested that dielectric and electrical properties, for example dielectric loss of doped nickel ferrite is observed to decrease and resistivity is observed to increase by doping with transition metals [47].

### **2.3 Chemical co-precipitation method**

“The co-precipitation method has the ability to synthesize nano particles, involving complex oxides and electro ceramics, in a very short time. Fumes are generally emitted in this process which can be considered as a disadvantage. The process of growth, nucleation, agglomeration and coarsening is happening simultaneously in the reaction process. The nucleation involves the initial formation of large amount of small sized crystallites. As these small sized crystallites are thermodynamically unstable so they make aggregates to stabilize themselves. This phenomenon is known as growth. During coarsening, small particles add up with large particles. This happens in the growth process. The synthesis of nanoparticles requires a relatively fast nucleation process as compared to growth process [48].

The oxide can be synthesized by two methods. One type of reaction directly produces oxides and other type of reaction produce precursor that require more processing. On addition of alkaline solution the respective metal hydroxides forms and precipitates out in water. The alkaline solution can be potassium hydroxide, sodium hydroxide etc. The resulting solution mixture is washed many times with deionized water until its pH value reaches to 7. The chloride ions are washed away. The resulting neutral solution is dried and calcinated in order to obtain the final product. The final product usually has a nano size. Co-precipitation method is a good method for production of ferrites that are pure and chemically homogenize. The oxide nano particles can be obtained by salts like nitrates, sulphates and chlorides. The size of the synthesized particles depends on various parameters like molarity and pH of precursor. The transport rate is affected by chemical concentration. The crystallinity is affected by impurities and reaction rate. Nucleation, growth rate and super saturation have an effect on particle's shape and size. The size of particle is small at high super saturation and particles have large size at low super saturation. The most commonly used precipitating agent is sodium hydroxide [49]. A specific value of temperature and pH is required for the reaction to proceed.” The co-precipitation process is shown in Fig.

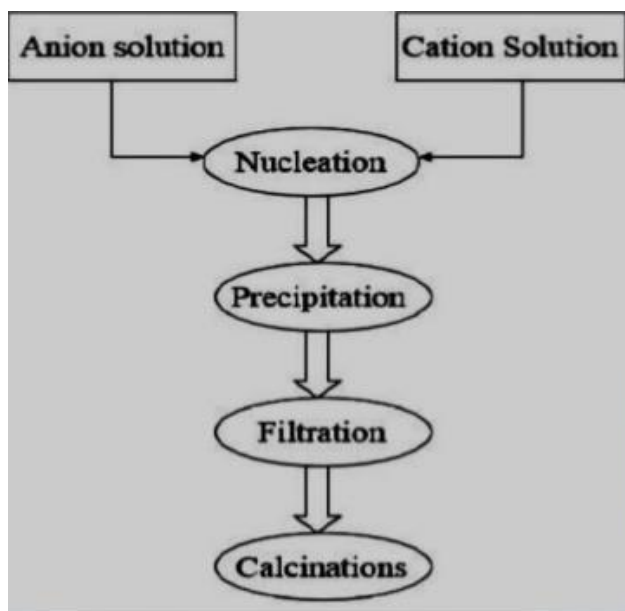


**Fig 2.1 Steps involved in co-precipitation method [50]**

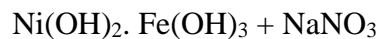
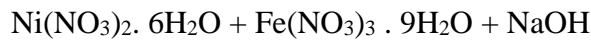
### 2.3.1 Prime steps in co-precipitation

Co-precipitation reaction involves two main steps which are as follows.

- Co-precipitation step
- Ferritisation step

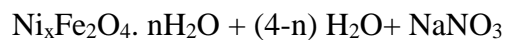
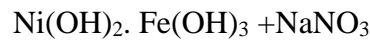
#### 2.3.1.1 Co-precipitation step

Firstly the metal ions co-precipitate in the basic medium. As a result colloidal particles of solid metal hydroxides are obtained. Following will be the reaction procedure in case of Ni ferrites.



#### 2.3.1.2 Ferritisation step

The product obtained through co-precipitation step is heated in alkaline medium. As a result metal hydroxide solution gives Ni ferrites.



There are a lot of parameters that affect the shape and size of the resultant products nano particles. Washing of sample is done several time using deionized water until the pH of solution reaches to 7. The washing also removes impurities to a large extent.

## 2.4 Variables include in co-precipitation method

Following are the factors effecting co-precipitation process:

- Role of anion
- Rate of mixing of the reactants
- Effect of pH
- Temperature effect
- Heating after co-precipitation

#### **2.4.1 Part of anion**

The type of anion utilized during the process has a special and important effect on the properties of resulting product nano particles. Salts or solution of metal ions are the sources that provide anion. The metal salts gives the best results that's why it is usually recommended to use metal salts like chlorides, nitrates etc.

#### **2.4.2 Speed of blending of the reactants**

The size of the resultant product nano particles depends greatly on the rate at which the solution is stirred. Growth and nucleation are the processes that govern the size of particles formed during co-precipitation process. If growth rate is slow compared to nucleation rate then size of the product particles will be small. High growth rate can be achieved by fast stirring rate. On the other hand if growth rate is faster than nucleation rate then the size of the resultant product particles will be large. Low growth rate can be achieved by slow stirring. The particles will be chemically homogenized in case of slow mixing [51].

#### **2.4.3 Impact of pH**

The size and shape of the particle is greatly affected by pH of the solution. There is no significant particles growth at low pH value. The growth of particles significantly increases at high pH value. When the value of pH is increased the time needed for synthesis is decreased. In case of nickel ferrite the range of pH is 11-12.

#### **2.4.4 Temperature influence**

In case of ferrite formation, different metals have different activation energy values. The heat provided by reactants gives rise to activation energy. The reaction

temperature ranges from 80°C to 100°C in case of nickel ferrite formation in co-precipitation reaction.

#### **2.4.5 Heat treatment after co-precipitation process**

Annealing is needed for phase formation after the completion of co-precipitation reaction. The shape and size of particles considerably depends on amount of heat and the time period for which the heat is applied.

There are various advantages of co-precipitation method over other applicable methods.

- The resultant particles formed will be homogenous and mono dispersed.
- The preparation procedure is simple and efficient.
- Excellent controllability of shape and size of resultant particles.
- The composition of particles can also be well controlled.

#### **2.5 Synthesis of NiFe<sub>2</sub>O<sub>4</sub> nanoparticles**

In order to synthesize nickel ferrite nano particles the chemicals used were nickel nitrate (Ni(NO<sub>3</sub>)<sub>2</sub>.6H<sub>2</sub>O) and iron nitrate (Fe(NO<sub>3</sub>)<sub>3</sub>.9H<sub>2</sub>O). Sodium hydroxide (NaOH) was used to maintain to pH of solution around 11-12. The pH is maintained at 7 by washing the resultant nano particles with deionized water several times. Following stoichiometric formula was used in order to calculate composition of different chemicals utilized in the process.

$$\text{Mass} = \text{Molarity} \times \text{Molecular Mass} \times 100$$

$$1000$$

The starting materials for the reaction were nickel nitrate (Ni(NO<sub>3</sub>)<sub>2</sub>.6H<sub>2</sub>O) provided by ACROS Organics, iron nitrate (III) nonahydrate (Fe(NO<sub>3</sub>)<sub>3</sub>.9H<sub>2</sub>O) provided by EMSURE® Merck KGaA Darmstadt Germany (99% purity), sodium hydroxide (NaOH) provided by FischerChemical Ltd. – Hong Kong and graphene platelets provided by Sigma Aldrich. All the materials were analytical grade. Nickel nitrate, sodium hydroxide (3M) and iron nitrate were dissolved in stoichiometric amount in 200 ml of deionized water. Each solution was magnetically stirred for ten minutes. Deionized

water was used as a solvent to minimize the presence of impurities in final product. The solutions of nickel nitrate and iron nitrate were mixed together and magnetically stirred for 30 minutes at room temperature for homogenous mixing. The nitrates solution was heated under constant stirring up to 90 °C. The solution of precipitating reagent, already heated at 90 °C, was mixed with the nitrates solution under constant stirring at the temperature of 90 °C. Both solutions were heated at 90 °C for 45 minutes under constant stirring. At room temperature the pH of the solution was maintained at 12. Deionized water was used for thoroughly washing the precipitates in order to obtain impurity free nickel ferrite nanoparticles. The water content was removed by drying the product in electric oven overnight at the temperature of 100 °C. The dried product was calcinated in muffle furnace for seven hours at 800 °C.

## **2.6 Synthesis of nickel ferrite/graphene platelets nano-composite**

The nano composite of nickel ferrite and graphene was prepared using ultrasonic method. Different percentage of graphene platelets (5%, 10%, 15%, 20%) were added in to 50 ml of deionized water. The mixture was sonicated for 6 hours at room temperature. Afterwards nickel ferrite nanoparticles were added in the solution and the solution was sonicated for 6 hours at room temperature. The solution was dried over night at 100 °C. The agate mortar and pestle was used for the homogenized mixing of dried powder. The pallets were prepared using hydraulic press. The load of 40 kN was applied for 4 minutes on each pallet. The pallets were annealed at 400°C for one hour. Magnetic and electric measurements were obtained using these prepared pallets.

Standard techniques were used for the characterization of prepared samples. By utilizing Stoe Diffractometer system with CuK $\alpha$  radiation (1.5405 Å) at room temperature, XRD pattern of each powdered sample of nickel ferrite/graphene composite was recorded in the 2 $\theta$  range of 20°-80°. XRD provided information about structural and phase of prepared nano composites. By using Perkin Elmer Spectrum FTIR spectrometer, FTIR analysis was performed. The KBr pallets were used to find out vibration bands of metal oxygen in the range of 350-4000cm<sup>-1</sup> in nickel ferrite/graphene nano composite. Microstructure analysis and surface study was performed using JEOL JSM (model no.6390) scanning electron microscopy (SEM). The SEM was performed

by dissolving a very small amount of powdered product in deionized water and sonicated for two hours. Wayne Kerr Precision Impedance analyzer (Model No.6500B) was used for the investigation of dielectric properties at room temperature.

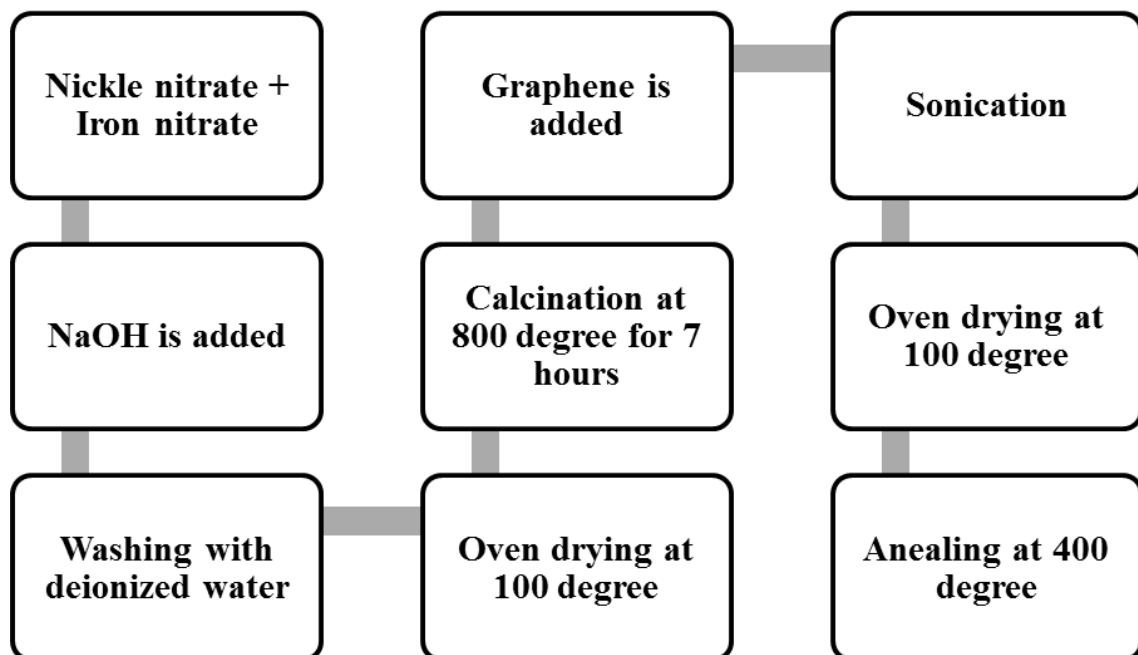


**Fig 2.2 Synthesis process**

## **2.7 Water as a dispersive medium**

The water is polar in nature. This polarity makes water a good solvent medium for ionic or polar solutes. Water molecules surround the ionic or polar molecule as it enters the water. This process is known as hydration. One solute molecule is surrounded by many water molecules as the size of water molecules is small. The partially negative end of water molecule is attracted towards partially positive end of solute molecule. This is known as hydrogen bonding.

The sodium chloride salt is an example of ionic solute. It splits in to cations and anions and these ions are surrounded by water molecules. In this way these molecules are carried away from there crystal lattice in to solution. Sugar is an example of non-ionic

solute. The dipole region of sugar molecules makes hydrogen bonding with water dipoles. In this way sugar is mixed in to solution.



# Chapter 3

## Introduction to sample characterization techniques

The properties of synthesized nickel ferrite nanoparticles with graphene loadings are analyzed by performing some specific analysis techniques. Properties like physical and chemical properties and other information about material such as morphology, lattice parameter, structure etc. can be obtained using one of the analysis techniques. This chapter will cover a short introduction of the characterization techniques. Following characterization techniques can be used for the analysis of synthesized composite.

### 3.1 X-Ray diffraction technique

It is a useful tool for the identification of degree of crystallinity and structure of a material. Clear information about structural strain, crystal defects, average crystallite size, crystallographic orientation and degree of crystallinity can be obtained by using XRD. Three different methods can be used for finding out crystal structure i.e. powder diffraction method, Laue method and rotating crystal method. Two techniques can be used to determine crystal size if powder diffraction method is used. Those techniques are as follows.

- Debye Sherrer Method
- Diffractometer method

The sample was in the form of fine grinded powder. Copper, Molybdenum etc. can be used as a target material. Cu-k $\alpha$ =1.54 source was the XRD source used for analysis in this case.

### 3.1.1 Basic principle of XRD

The powdered sample is placed for analysis. X-ray beam is made to fall on the sample and reflected from plane of crystal. The crystal plane reflects the X-rays that are incident on material. The interference only takes place when incidence angle is exactly same as reflection angle. The Bragg's Law is given by

$$n\lambda = 2d\sin\theta \dots\dots\dots(3.1)$$

$n$  is order of interference,  $\theta$  is incidence angle,  $d$  is Interlayer distance and  $\lambda$  is incident X-ray wavelength. The Bragg's law states that the incident ray is reflected only when the path difference between set of planes is  $2d\sin\theta$  [52]. The set of planes are at an equal distance of  $d$ . Following is the condition required for constructive interference:

$$2d\sin\theta = n\lambda, \text{ where } n=1,2,3,\dots$$

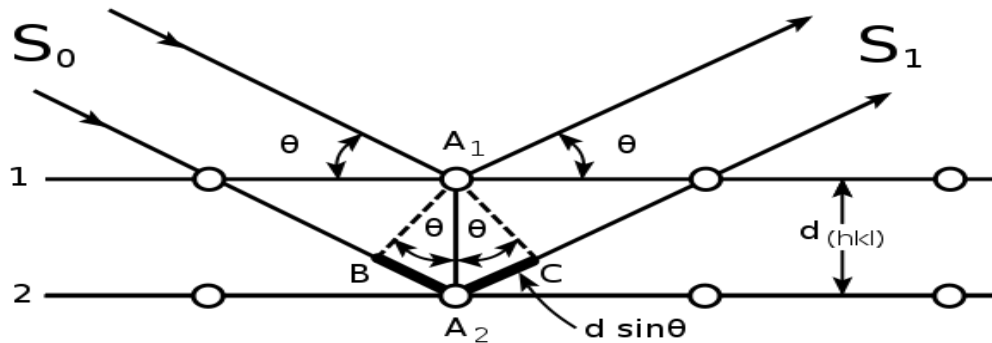


**Fig 3.1 Incident x-ray beam scattered by atomic plane in a crystal [53]**

The equation is known as Bragg's equation. The condition for reflection in above mentioned equation is that it only occur when  $\theta < 2d$ . For this reason visible light cannot be used. For the characterization of a three dimensional structure three techniques are usually used which are as follows:

- Laue Method
- Powder method
- Rotating Crystal Method

The sample which is to be characterized using XRD is in the form of Nano powder. So the powder method will be the one useful for the desired sample. For the evaluation of powdered sample and in the case of in availability of single crystal of acceptable size, powder diffraction is the best method to be employed. The procedure of this experiment includes the crushing of sample in to fine powder. Afterwards the sample will be placed in aluminum or glass rectangular shaped plate. A monochromatic X-ray beam is then directed towards the powdered sample.

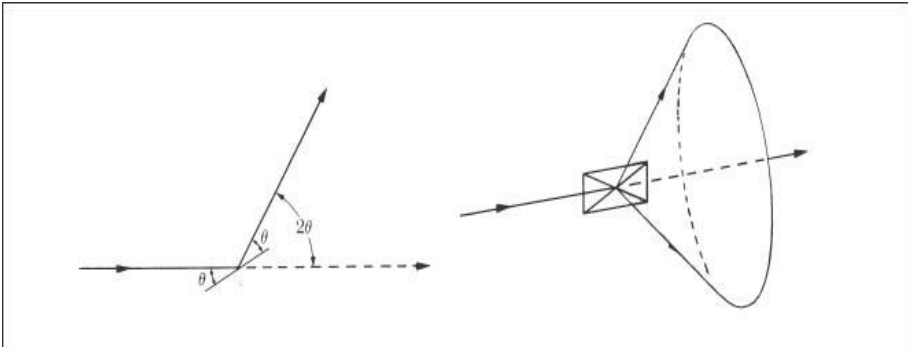


**Figure 3.2 Diffracted cones of radiations forming in powder method [53]**

Consider the reflection as shown in figure. The fraction of sample, which is in powder form, is at such an orientation which will enable reflection by being present at correct Bragg angles. When the plane is rotated about the beam which is made incident, the path of motion of reflected beam will be across the surface of cone. In the case of our particles the reflection does not occur across the surface, a large number of crystal particles will have same reflections and some of those reflections will be able to satisfy brags law. The inter planner spacing, d, can be calculated by knowing values of  $\lambda$  and  $\theta$ .

- **Lattice constant**

Lattice constant defines the unit cell of a crystal. It is the length of one edge of the cell or an angle forming between edges. It can also be termed as lattice constant or lattice parameter. The distance, which is constant, between the lattice points is known as lattice constant. Following equation is used to calculate lattice constant.

$$a = \frac{\lambda (h^2 + k^2 + l^2)^{1/2}}{2 \sin \theta} \dots \dots \dots (3.2)$$

In the above equation, lattice constant is “a”, the wavelength of X-ray radiation is 1.54 for  $Cu\alpha$ , miller indices are “h, k, l” and diffraction angle is  $\theta$ .

- **Crystallite size**

For the identification and confirmation of the experimentally obtained diffraction pattern it is compared to JCPDS cards. The structural properties are greatly influenced by particle size. According to Debye Sherrer equation, which is used to calculate particle size, crystal size is inversely proportional to peak width. So the small crystallite size is related to peak broadening in XRD analysis. The Debye sherrer equation is used to calculate particle size.

$$t = \frac{0.9 \lambda}{\beta \cos \theta} \dots\dots\dots(3.3)$$

$\lambda$  represents the incident X-ray wavelength and  $\theta$  and  $\beta$  represent diffraction angle and full width half maximum respectively.

- **X-Ray density**

The X-ray diffraction data can be used for the calculation of sample material’s density [54]. If the lattice constant is known for each sample following formula will be used.

$$\rho_x = \frac{8M}{Na^3} \dots\dots\dots(3.4)$$

Where  $\epsilon$  represents molecular weight of sample, N is the Avogadro’s number ( $6.03 \times 10^{23}$ ) and "a" is the lattice constant. Eight formula units are possessed by each cell.

- **Measured density**

The intrinsic properties of materials define the bulk density or measured density. The density formula is generally used for the density calculation.

$$\rho_m = \frac{m}{\pi r^2 h} \dots\dots\dots(3.5)$$

Where m represents the mass, r represents the radius; h is the thickness of the pressed pellet sample.

For the calculation of measured density, a circular pallet is made using hydraulic press which compact the powdered sample. Vernier caliper is used for measuring thickness and radius of pallet and analytical balance is used for measuring mass of the pallet. The measured parameters are substituted in equation for the resultant density calculation.

- **Porosity fraction**

Along with the alternation in compositions, the increase in the porosity fraction is observed. Following formula is used for calculation of porosity fraction.

$$\text{Porosity Fraction} = 1 - \frac{\rho m}{\rho x} \dots\dots\dots (3.6)$$

### **3.2 Scanning electron microscopy**

Scanning electron microscopy is an imaging technique which makes use of high energy electron beams for imaging Nano and bulk surfaces. When the highly energetic beam strikes the sample surface it provides following information.

- Composition of the sample.
- Phase mapping
- Topography of the sample.

When the beam hits the surface of material there will be various kind of interactions and signals are emitted as a result of these interactions such as transmitted electrons, back scattered electrons, secondary electrons, cathodoluminescence and characteristic X-rays [35].

#### **3.2.1 Basic principle of SEM**

The beam of electron is made to focus on the surface of sample in scanning electron microscopy. The raster scan is used which can focus on very narrow cross sectional area. The surface of sample will emit electrons or photons when the incident

electron beam interacts with the surface. Different sets of detectors are employed to collect the emitted photons and electrons. The brightness of the cathode ray tube is controlled by using the outputs of detectors. The X and Y input of cathode ray tube are adjusted in relation with X and Y voltages rastering the beam of electron. As a result image is obtained on cathode ray tube display. Images are produced by backscattered electrons, elemental x-rays and secondary electrons.

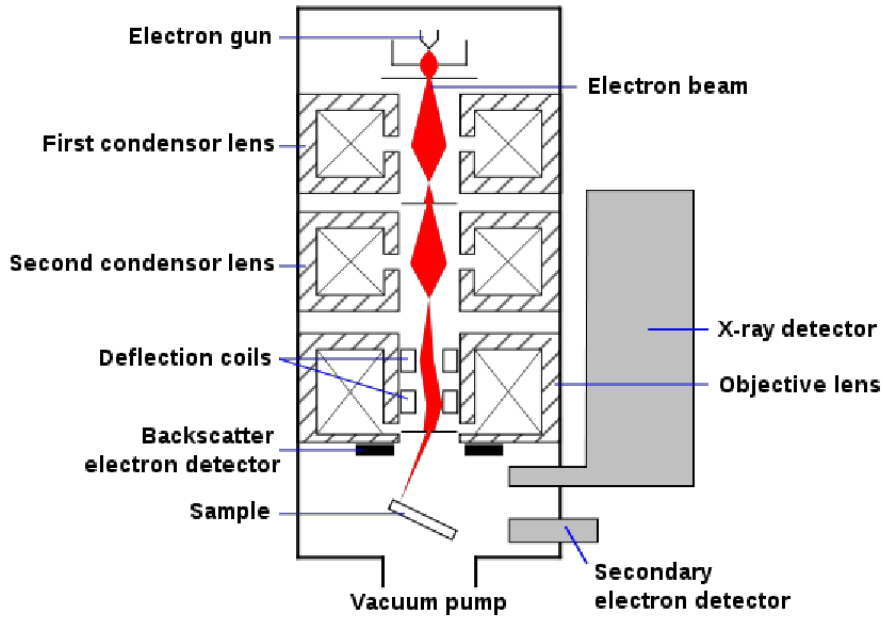


**Fig 3.3 Schematic figure of scanning electron microscope [55]**

### **3.3 Fourier transform infrared spectroscopy**

The absorption, emission spectra's, Raman scattering and photoconductivity of the material can be obtained by using this analytical technique. The stretching modes of the elements present in composite and chemical purity of the sample can be determined using FTIR. It is known as FTIR because it involves the Fourier, a mathematical term. It collects the data from spectrum of matter. FTIR is used to determine the amount of light that a sample absorbs at a specific wavelength.

### 3.3.1 Working of FTIR

In FTIR, an infrared light beam from a source which is polychromatic is made to fall on splitters. Half portion of the incident light is refracted towards fixed mirror and other half of the incident light is transmitted through a moving mirror. Transmitted light pass through the sample. The information about molecular component and structure of the sample can be obtained by interaction of light with sample.

### 3.3.2 Applications of FTIR

A gas chromatograph is used to separate the components of a mixture

- The analysis of liquid chromatography fraction can be done using FTIR.
- Tiny samples can be checked with the help of infrared microscope in sample chamber.
- The sample acquiring emitted spectrum of light is obtained FTIR instead of light spectrum through the sample [24]

## 3.4 Electrical properties

### 3.4.1 Dielectric properties

The LCR meter bridge is used for determination of dielectric properties such as dielectric loss, dielectric constant etc. Firstly the capacitance of pellets were find out using LCR meter then following formula is used for the calculations of dielectric constant.

$$\epsilon' = \frac{Cd}{A\epsilon_0} \dots\dots\dots(3.7)$$

Where C represents the capacitance of the pellet (farad), t represents the thickness of the pellet (Meters), A represents the cross-sectional area of the flat surface of the pellet and  $\epsilon_0$  is the constant of permittivity for free space and its value is equal to  $8.85 \times 10^{-12}$  F/m. The imaginary part that corresponds to the energy dissipation losses is calculated by using the following equation:

$$\epsilon'' = \epsilon' * D \dots\dots\dots(3.8)$$

There will be some power losses in dielectric materials. These losses are due to the work done in order to overcome frictional and damping forces faced by dipoles during their rotatory motion. The dielectric loss tangent can be found out by using following equation.

$$\tan \delta = \frac{\epsilon''}{\epsilon'} \dots\dots\dots (3.9)$$

Following equation is used for calculation of AC conductivity:

$$\sigma_{ac} = \omega \epsilon \epsilon_0 \tan \delta \dots\dots\dots (3.10)$$

**3.5 Reflection Loss:**

The interference that takes place as a result of struction of incident wave with the medium used for absorption is called microwave absorption. Inductance, resistance and capacitance are the properties that are used to find out the nature of above interaction. The reflection loss of a material is the result of all the previously mentioned factors. In case of induction of current in system, the induced current will consume energy. As for insulating material the presence of induced currents can be neglected because for induced currents a cross between crystal grains is necessary. The nature of interaction between electromagnetic radiations and material can be described using inductance and capacitance. Also the permittivity and permeability plays an important role. The permittivity of the material is the ability of material to store energy in the electric field. This stored energy will stay stored in the material until it is utilized to do some electrical work. The dielectric is a material placed between two plates of capacitor. It can be air, polymer etc. the presence of dielectric keeps the charges separated and also it increases the charge storage capacity of capacitor. The dielectric aligns the dipoles and allows them to do electric work in presence of electric field.



# Chapter 4

## Results and Discussions

### 4.1 X-ray diffraction Results

The knowledge of phase formation and exploration of structure was obtained using XRD. The prepared sample was finely ground and annealed before subjecting it to XRD.

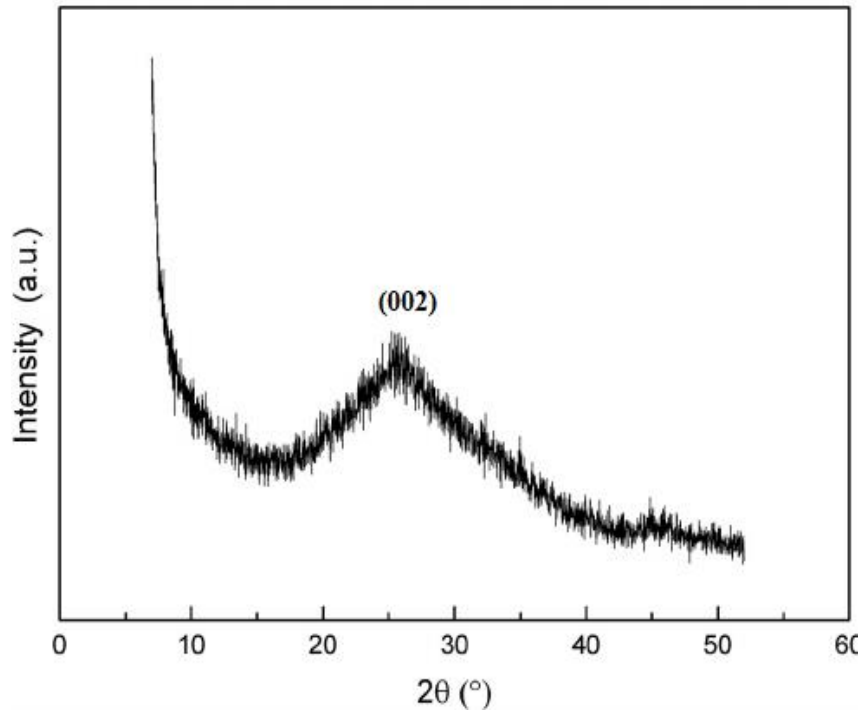


**Fig 4.1 XRD pattern of pure graphene platelets**

Fig 4.1 shows the obtained XRD patterns at room temperature. The nicely separated diffraction peaks appears for all the samples at planes (2 2 0), (3 1 1), (4 0 0), (5 1 1), and (4 4 0) present at the respective angles of  $2\theta = 30.1, 35.4, 43.2, 57.0$  and  $62.7$ . The presence of these peaks at specific angles verifies the generation of FCC spinel phases in relation to card number JCPDS 00-022-1086. The characteristic peak present at

$2\theta=26.0^\circ$  corresponding to plane (0 0 2) refers to the graphitic reflection of graphene. As the graphene content is increased the peak became more intense. This shows that the excess graphene does not penetrate the ferrite crystal lattice. It is uniformly dispersed on the surface of ferrite.

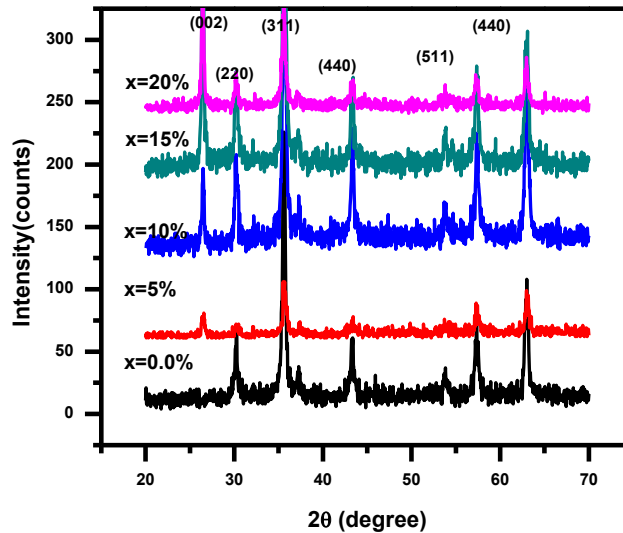


**Fig 4.2 XRD patterns of ferrites with increasing graphene platelets concentration**

The average crystallite size is calculated using Debye's Scherer formula for the most intense peak present at plane (3 1 1). The average size is in the range of  $26 \pm 6$  nm [56]. Fig 4.3 shows the trend of average crystallite size as a function of graphene concentration. The crystallite size decreases with increase in graphene concentration. This behavior can be attributed to increase in FWHM of respective peaks, as the conductive network formed by graphene and that is cutting through grains, hence causing decrease in crystallite size.

Fig 4.4 shows the trend of bulk density. The graph shows a decreasing trend in bulk density with increase in graphene concentration as the porous nature of graphene enhanced the general porous volume. Fig 4.4 also shows the trend of x-ray density. The decreasing trend is observed in x-ray density with increase in concentration of graphene. This is attributed to the high volume and low mass of graphene.

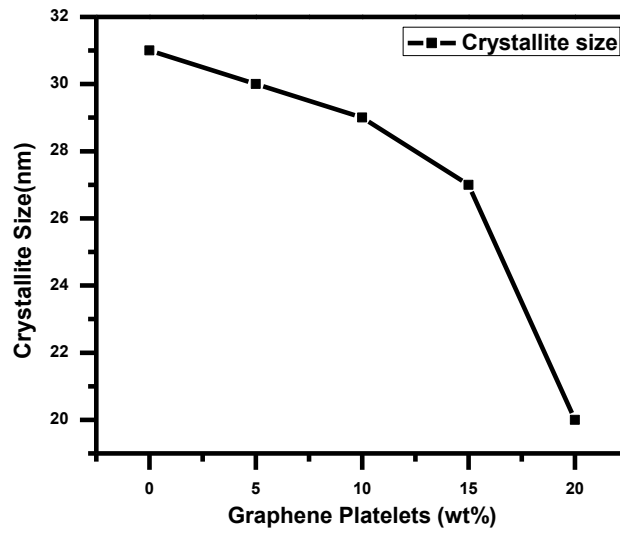


**Fig 4.3 Crystallite size variation with increasing graphene platelets concentration**

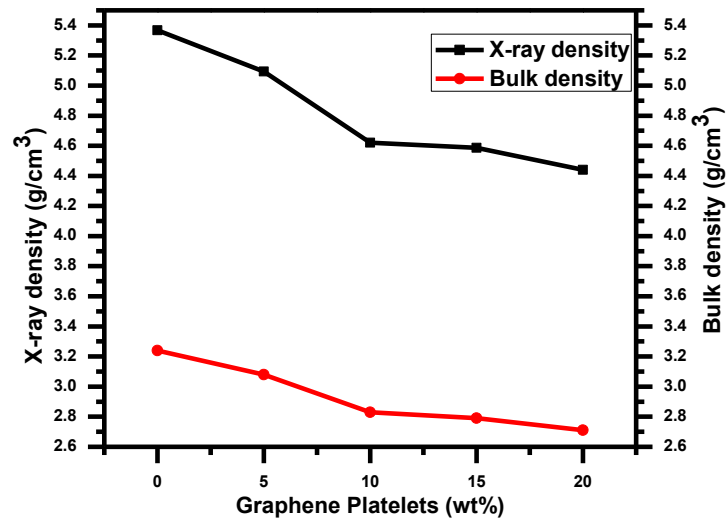


**Fig 4.4 Variation of x-ray and bulk density with graphene platelets weight %**

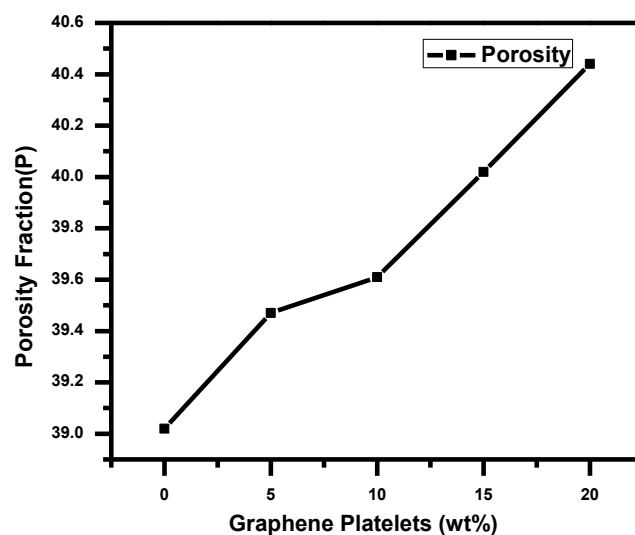


**Fig 4.5 Porosity fraction variation versus graphene platelets weight %**

Fig 4.5 shows the graph of porosity fraction. With increase in concentration of graphene the porosity fraction is increasing. The chances of presence of defects in grains increase with increased graphene content because graphene is porous and light in weight also due to increase of interface between graphene and ferrites.

## 4.2 Scanning electron microscopy results

Scanning electron microscope was used to find out  $\text{NiFe}_2\text{O}_4$  nano particles size and morphology and to see how nanoparticles are decorated on graphene platelets. The results are shown here. The results include pure  $\text{NiFe}_2\text{O}_4$ , Pure graphene platelets, and loading of graphene with ratio 5%, 10%, 15%, and 20%. All the results show the attachment of nickel ferrite nano particles on graphene sheets. For the morphological analysis of pure nickel ferrite and nickel ferrite/graphene composite, both the powders were annealed and a suspension in deionized water was made using sonication. This will allow nanoparticles to arrange in lowest interface energy configuration. Fig 4.7 shows the uniform distribution of pure nickel ferrite nano particles. The nano particles are fairly separated and distinguished from each other and the size ranges from 15nm to 25nm. Fig shows the attachment of nickel ferrite nano particles on graphene sheets.

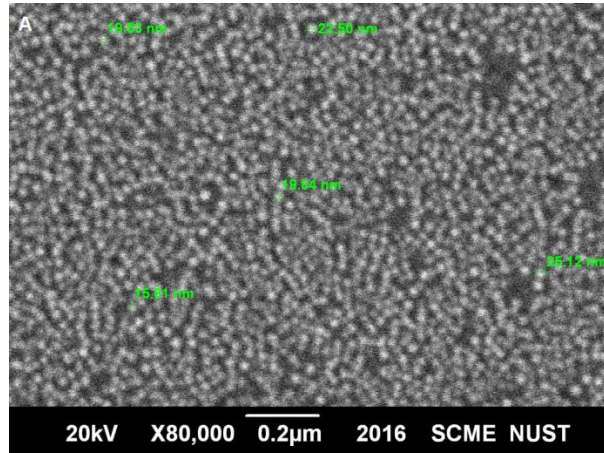


**Fig 4.6 SEM image of pure nickel ferrite**

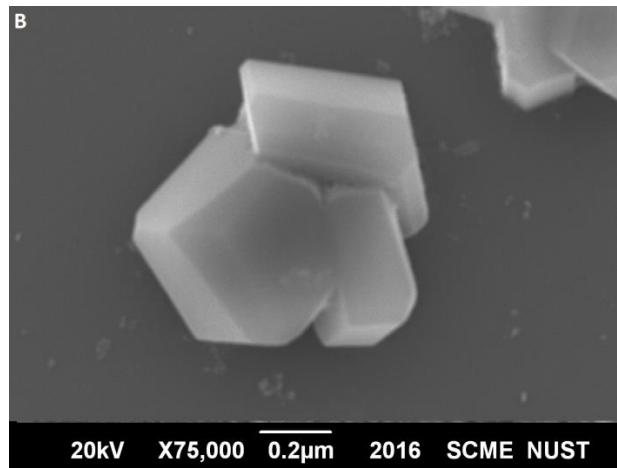


**Fig 4.7 SEM image of pure graphene platelets**

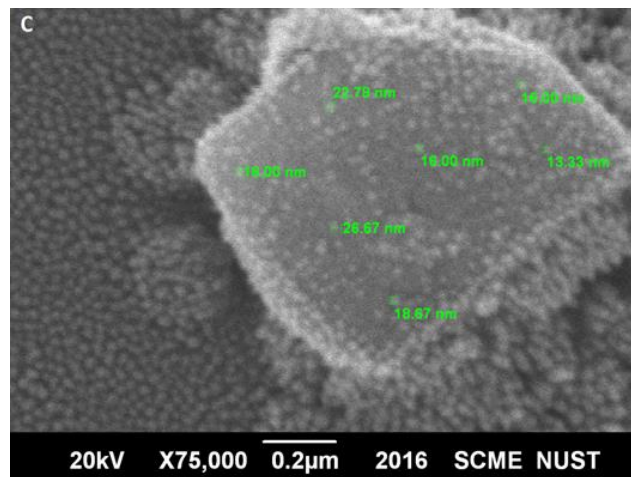


**Fig 4.8 SEM image of ferrite with 5% graphene Platelets**

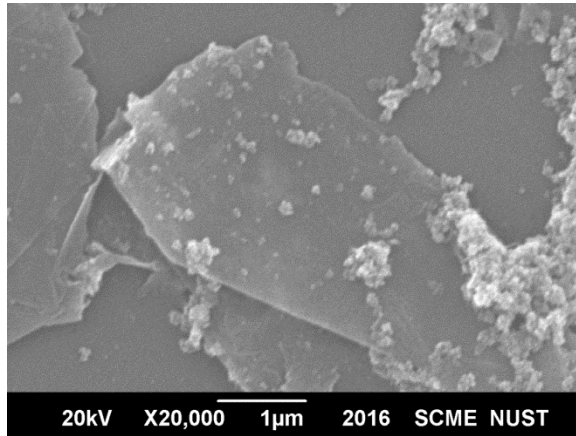


**Fig 4.9 SEM image of ferrite with 10% graphene platelets**

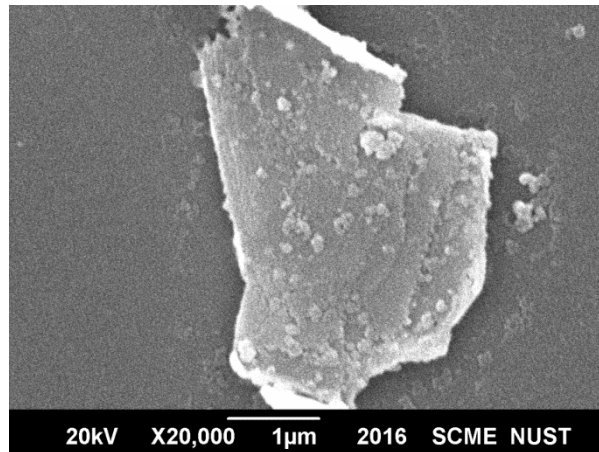


**Fig 4.10 SEM image of ferrite with 15% graphene platelets**

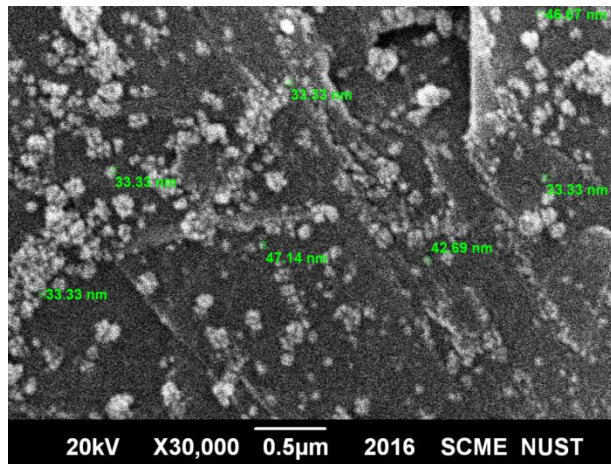


**Fig 4.11 SEM image of ferrite with 20% graphene platelets**

The size ranges from 16nm to 26nm. This shows the success of the experimental procedure involving dispersion.

### 4.3 Fourier transform infrared spectroscopy results

The Fig 4.12 shows the FTIR analysis of pure nickel ferrite and its composite with graphene. The KBr pallet is used and analysis is performed at room temperature in the range of  $300\text{ cm}^{-1}$  to  $1000\text{ cm}^{-1}$ . It can be inferred from the FTIR results that the same kind of chemical bonds are present in all the samples as the spectra shown by all samples are nearly undifferentiated. Similar kinds of results are reported by other research papers [52]. In ferrites the two sub lattice positions occupied by metal ions are tetrahedral and octahedral positions. These sub lattice positions give rise to absorption bands.

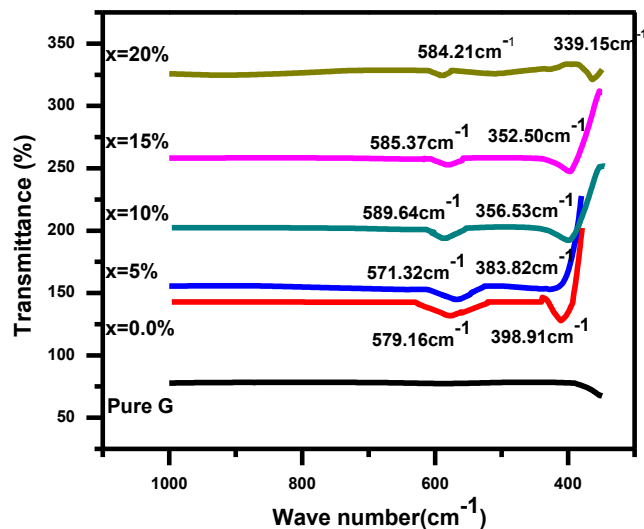


Fig 4.12 FTIR spectra of prepared ferrites

The bands at  $\nu_1$  ( $339\text{ cm}^{-1}$  to  $400\text{ cm}^{-1}$ ) and  $\nu_2$  ( $594\text{ cm}^{-1}$  to  $600\text{ cm}^{-1}$ ) refer to the presence of metal oxides. The peak at  $\nu_1$  and  $\nu_2$  respectively represent metal vibration in octahedral and tetrahedral complexes [52]. These bands will appear as a result of stretching of tetrahedral and octahedral lattice sites. The absorption bands appear as a result of stretching and vibration of metal-oxygen bonds at both lattice sites. Due to the variation in bond lengths of Fe-O, the position of bands differs slightly from each other at both tetrahedral and octahedral lattice sites [57].

## 4.4 Dielectric studies

To find out the dependence of dielectric constant, dielectric loss, tan loss, Ac conductivity and Ac impedance on frequency, pellets were prepared and sintered and standard relations are used for calculations [58].

### 4.4.1 Dielectric constant

The dielectric constant has a real and imaginary part. The real part deals with the ability of polarization or the extent to which a material can store energy. The dielectric constant of a material can be the result of dipolar, interfacial, electronic or ionic polarization [59]. As the frequency increases a decreasing trend of dielectric constant for each sample is shown in Fig 4.13. The values of dielectric constant for every sample became eventually constant at higher values of frequencies. The decrease in space charge polarization is the reason behind decreasing trend of dielectric constant. The decrease in space charge polarization is due to inability of dipoles to line up counter to sudden shift of applied electric field. The value of dielectric constant is high at low frequencies. Pure nickel ferrite has  $3.46 \times 10^4$  value of dielectric constant at 100Hz. However the value of dielectric constant has increased significantly for Nickel ferrite/graphene nano composite. Nano composite with 20% graphene has a dielectric constant value  $6.31 \times 10^{16}$  at frequency 100Hz. Maxwell and Wagner model of space charge polarization can narrate the amplification of dielectric constant values at low frequencies [38]. The model describes the separation of dielectric material by two layers, extremely resistively grain boundaries and effectively conducting grains. The electrons can effortlessly proceed towards the grain boundaries in presences of external field. The extremely resistive nature of grain boundaries results in charge accumulation that originates large polarization [60]. At low frequencies these charge carriers provide fast reaction to variations in electric field. This response contributes to polarization resulting in high value of dielectric constant. At higher frequencies the charge carriers provide slow response to the electric field variations.



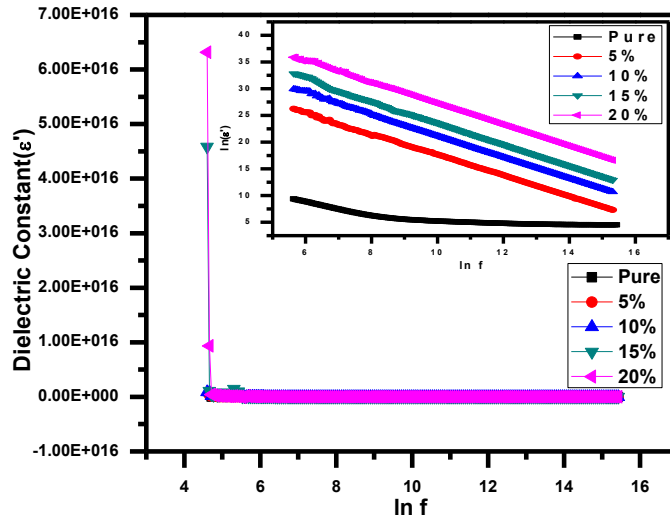


Fig 4.13 Variation of dielectric constant with frequency

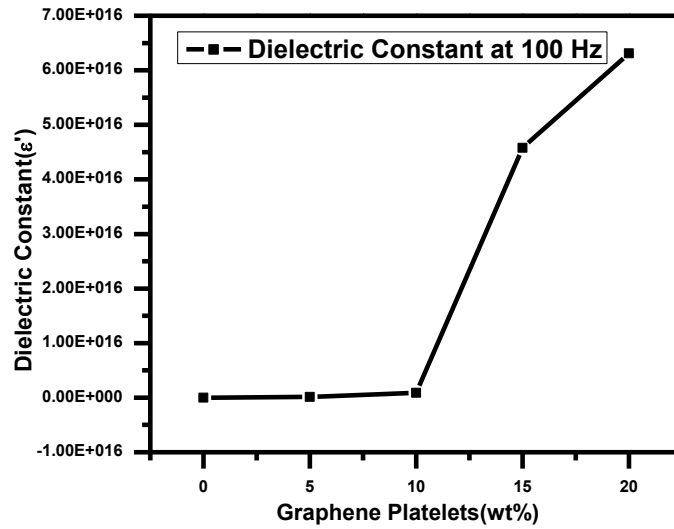


Fig 4.14 Dielectric constant at 100 Hz

This will result in decrease in dielectric constant as the polarization also decreases [60]. Graphene forms a conductive network and this will result in high aspect ratio and

increased conductivity. That's why dielectric values show a huge increase with addition of graphene content.

#### 4.4.2 Dielectric loss

Dielectric loss is the imaginary part that deals with the amount of energy dissipated [22]. The variation of dielectric loss with frequency is shown in Fig 4.15. A decreasing trend is observed in the values of dielectric loss with increase in frequency. The fig shows that values of dielectric loss increases significantly with increase in graphene content in nickel ferrite/graphene composite. The value of dielectric loss is higher at lower frequencies and its value decreases as the frequency increases. The value rises from  $5.28 \times 10^2$  for pure nickel ferrite sample to  $2.86 \times 10^{16}$  for sample having 20% graphene along with nickel ferrite. The Koop's theory clearly describes the behavior of dielectric loss. The theory states that in the low frequency regions the grain boundaries are extra resistive. As a result polarization requires a greater amount of energy. This will cause high energy losses. The grain boundaries are not so much resistive in the regions having high frequencies.

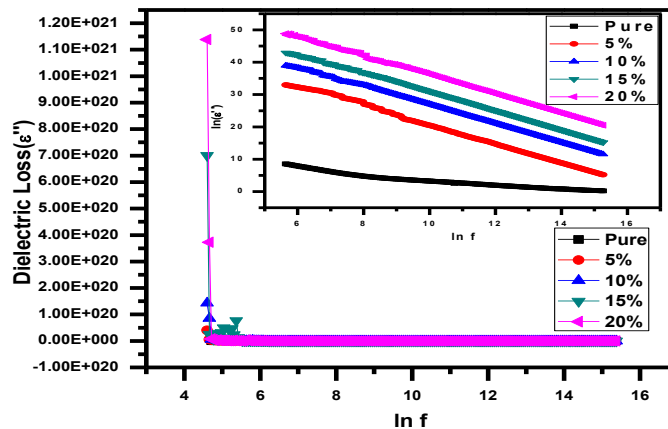


**Fig 4.15 Variation of dielectric loss with frequency**

The energy loss is slight as polarization requires less amount of energy. The value of dielectric loss has increased by adding graphene concentration in nickel ferrite.

This behavior is seen due to large specific surface area of graphene that will cause an increase in number of interfaces and voids present between graphene and nickel ferrite. These materials are fit for energy storage devices due to the values of dielectric loss and dielectric constant in the regions of high frequency and compact values of resistivity [61, 62].

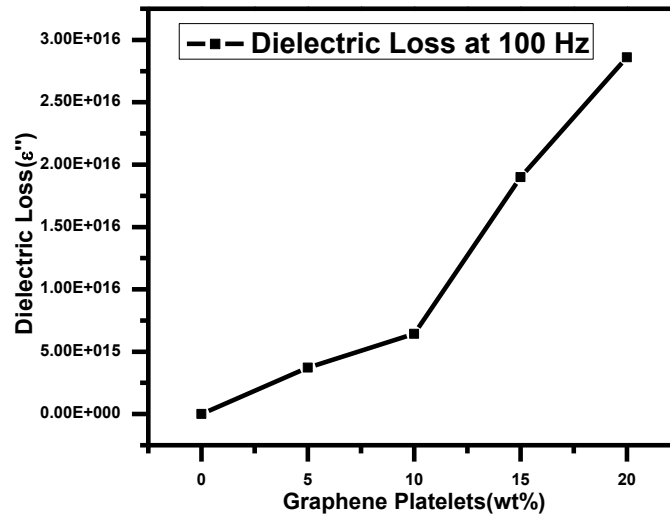


**Fig 4.16 Dielectric loss at 100 Hz**

#### 4.4.3 Dielectric tangent loss

The ratio of dielectric loss to dielectric constant is given by dielectric tangent loss. It quantifies the relative energy loss across a large frequency range due to varying electric field. The dielectric tangent loss shows a decreasing trend with increase in frequency in Fig 4.17. The increase in graphene content in nickel ferrite/graphene composite will give higher values of dielectric tangent loss at low frequencies. This increase in dielectric tangent loss values are in accordance with koop's theory. The theory explains that at lower frequencies the hopping of electrons is high. This hopping decreases at higher frequencies [61].

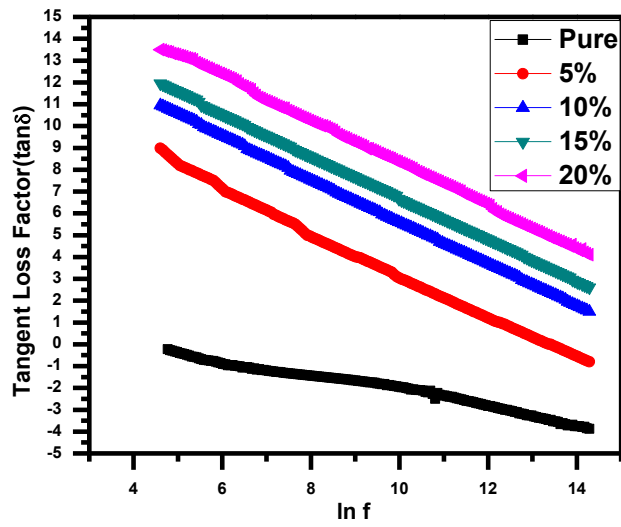


Fig 4.17 Variation of dielectric tangent loss with frequency

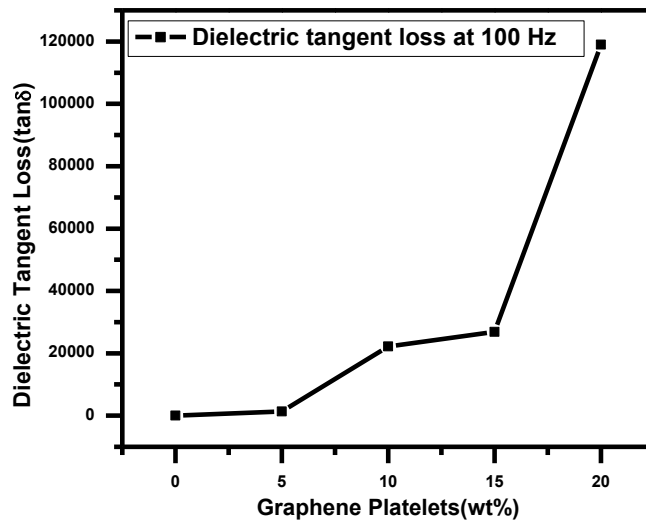


Fig 4.18 Dielectric tangent loss at 100 Hz

#### 4.4.4 Variation of AC conductivity

The trend of AC conductivity with frequency is shown in Fig 4.19. Following relation was used for finding out variation in AC conductivity of nickel ferrite/graphene nano composite.

$$\sigma_{ac} = \omega \epsilon_0 \epsilon' \text{Tan} \delta$$

Where  $\omega = 2\pi f$ ,  $\epsilon_0$  represents the permittivity of free space,  $\text{Tan} \delta$  represents the dissipation factor and  $\epsilon'$  represents the dielectric constant [63].

The Fig 4.19 shows an increasing trend of AC conductivity for pure nickel ferrite sample. In case of nano composite of nickel ferrite and graphene the AC conductivity shows a decreasing trend for 5%, 10%, 15%, 20% composition. The hopping mechanism of charge carriers causes the increase in conductivity with increase in frequency. The conductive nature of graphene can be considered as a reason for the decreasing trend of AC conductivity. Also another reason can be the increase in band gap width at nano size level, i.e. as the size of particle decreases the width of band gap increases. The following equation shows a direct relation between dielectric loss and AC conductivity.

$$\sigma_{AC} = \omega \epsilon_0 \epsilon''$$

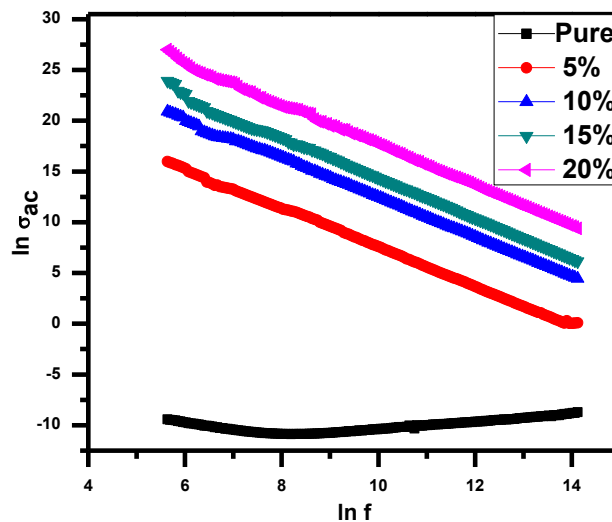
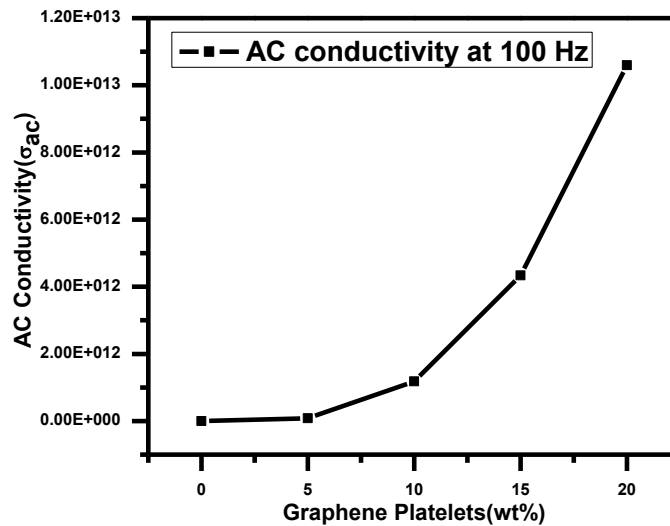


Fig 4.19 Variation of AC conductivity with frequency

The presence of higher percentages of graphene content causes increase in its conducting nature and as a result in low frequency regions hopping conduction and band conduction increases. The increase in the value of AC conductivity with increase in graphene content at low frequency values is due to the band conduction of garphene and hopping conduction of octahedral sites. At high frequencies, due to prompt increase in applied field, the decrease in AC conductivity is observed because the conductive nature of graphene obstructs the hopping mechanism [64].



**Fig 4.20 AC conductivity at 100 Hz**

#### 4.4.5 AC impedance

The size, microstructure and shape of nano materials have a direct effect on thermal properties. The information about microstructure can be obtained using impedance analysis. The imaginary and real components of conductive materials can be studied using impedance analysis. The impedance analyses of all synthesized samples were recorded in response to frequency. All of these measurements were performed at room temperature. The standard equations were used for the calculations [47].

The decreasing trend of impedance is show in in Fig 4.21 with increase in graphene content. The decrease in resistance is observed due to the increased conductivity near grain boundaries by adding graphene in nickel ferrite. The value of  $z'$

for pure nickel ferrite is  $1.36 \times 10^{14}$  and it is minimized to  $1 \times 10^{10}$  for 20% graphene content. The decreasing trend in value of  $z'$  proclaims an increase in conductivity which will result in decrease in resistance. The lower values of frequencies correspond to high impedance values. This is due to the factor of space charge polarization. It will render electron hopping inept to continue with the alternations of electric field. The impedance values became constant at higher frequencies due to the reduction in space charge polarization effect [65, 66].

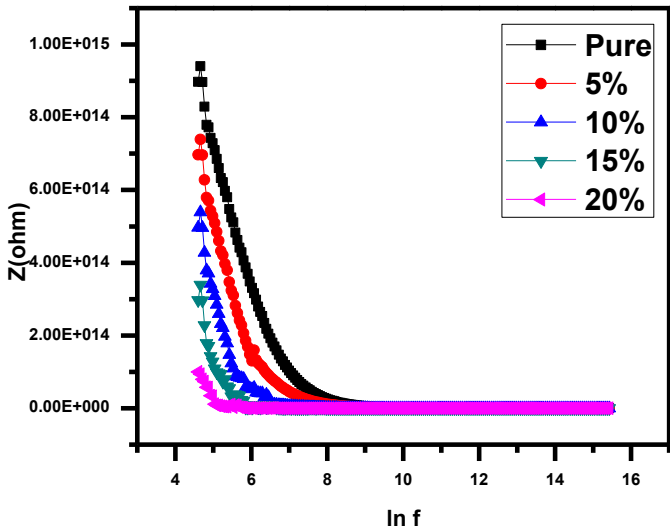


**Fig 4.21 Variation of impedance with frequency**

Fig 4.22 shows the Cole-Cole plot of Nickel ferrite and its composite with graphene at concentration of 0.0%, 5%, 10%, 15%, and 20%. The Fig 13 shows semi curved lines for each composition at specific frequency. The decrease in resistance is observed as in low frequency region grain boundaries are functional and grains are effective in high frequency regions. The decrease in length of lines with increase in graphene concentration shows a decrease in resistance. The pure nickel ferrite has highest value of grain boundary resistance ( $R_g$ ). The value of grain boundary resistance decreases with increasing graphene concentration. Nickel ferrite composite with 20% graphene shows the lowest value of grain boundary resistance. The lower values show the decrease in resistance due to increased conductivity and hopping mechanism. The

Cole-Cole plot of nickel ferrite/graphene nano composite is not a complete semi-circle due to the grain boundary resistance. This will confirm that the conduction is mainly due to grain boundaries [36, 67].

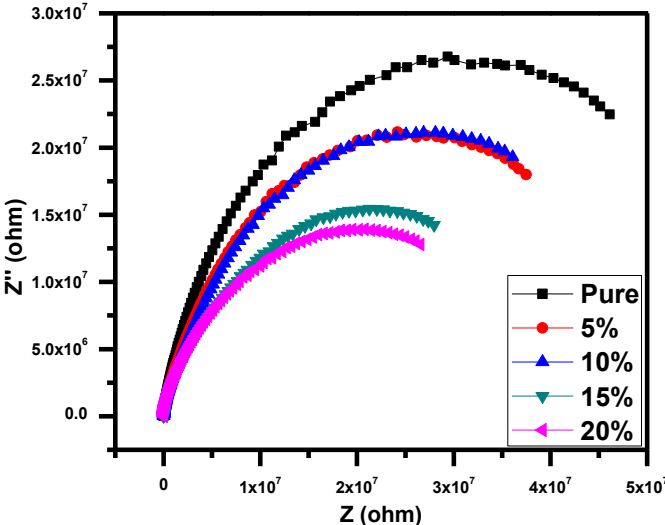


Fig 4.22 Cole cole plot of impedance

4.5 AC response of the material

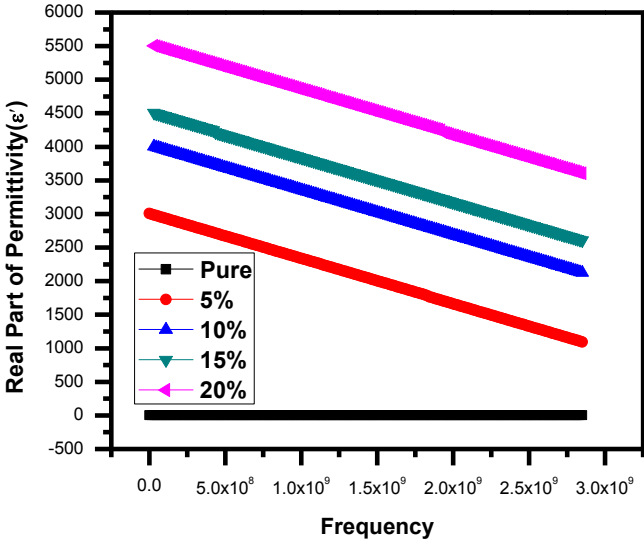
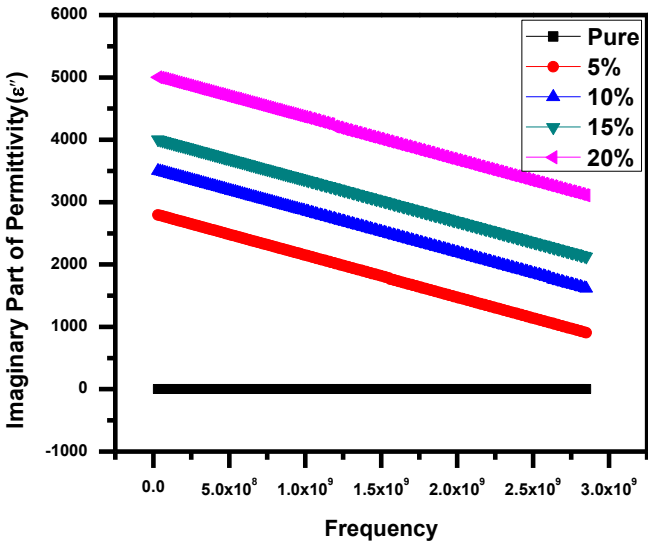


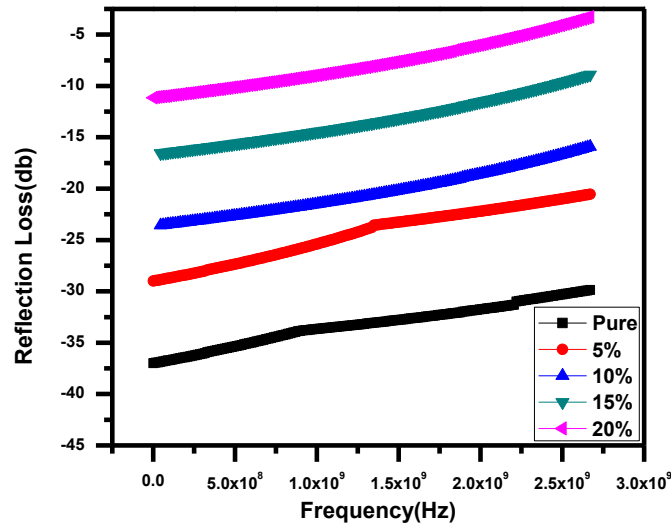
Fig 4.23(a) Real part of permittivity



Complex parameters like permittivity are used to show the behavior of material in presence of applied alternating field. Ferrites have remarkable dielectric nature so they are used as functional materials. The parameters that affect the complex permittivity in ferrites include size of grain boundary and grains and the distribution of cations [68]. The behavior of real and imaginary part of permittivity is plotted in Fig 4.23(a,b) as a function of frequency. Both  $\epsilon'$  and  $\epsilon''$  show a decreasing trend with increase in frequency. The values are high in low frequency regions and values decrease in regions of high frequency. This is a normal behavior associated with semiconductors. This is in accordance with Debye dielectric dispersion. The factors affecting dielectric polarization includes sintering time and temperature, substituting cation's type and the method used for preparing the materials [69]. Maxwell and Wagner [70] model can describe this trend of permittivity in non-homogenous materials on basis of grains and grain boundaries. According to Koop's theory, conductive grains are present in ferrites which are separated by grain boundaries that are resistive in nature [60]. Electron exchange phenomena govern the conduction in ferrites. The electrons arrive at grain boundaries due to hopping and gather there and this will result in polarization in low frequency regions. In high frequency regions, the electrons cannot cope up with alternating field so the trend of both real and imaginary part becomes steady.



**Fig 4.23(b) Imaginary part of permittivity**



#### 4.24 Reflection loss as a function of frequency

Reflection loss is a method for measuring microwave absorbing properties of material. The interaction of incident wave with absorbing media will give rise to the phenomena of microwave absorption. In case of induced current in material, the resistance consumes energy but there is no path for the flow of this current. In case of insulating materials, the presence of eddy currents can be over looked. The interaction between electromagnetic radiation and materials can be clearly understood by considering inductors and capacitors. Also the interactions can be characterized by considering  $\epsilon'$  and  $\epsilon''$  [39]. After the addition of graphene platelets in nickel ferrite nano particles, the processes of relaxation and polarization results in dissipation of energy. Furthermore, multiple scattering is faced by electromagnetic waves due to the presence of additional interfaces formed by adding graphene platelets. As a result the width of absorption band increases. The reflection loss decreases with increase in graphene concentration. This can be attributed to the high electrical conductivity of graphene. This will result in reflection of electromagnetic waves from absorber layer surface. This can be concluded that the best microwave absorption properties optimum can be achieved by combining optimum amount of graphene platelets and nickel ferrite nano particles [71].

**Table 1: Shows the variation of Crystallite Size, Lattice Constant, X-ray density, bulk density and porosity and Octahedral band positions ( $\nu_1$ ) of NiFe<sub>2</sub>O<sub>4</sub>/graphene platelets nano composite.**

<b>Graphene Content</b>	<b>Crystallite Size(nm)</b>	<b>Lattice Constant(Å)</b>	<b>x-ray density (g/cm<sup>3</sup>)</b>	<b>Bulk density (g/cm<sup>3</sup>)</b>	<b>Porosity (%)</b>	<b><math>\nu_1</math> (cm<sup>-1</sup>)</b>
<b>0.0</b>	<b>31</b>	<b>8.35</b>	<b>5.36</b>	<b>3.24</b>	<b>39.02</b>	<b>398.91</b>
<b>5</b>	<b>30</b>	<b>8.36</b>	<b>5.09</b>	<b>3.08</b>	<b>39.47</b>	<b>383.82</b>
<b>10</b>	<b>29</b>	<b>8.33</b>	<b>4.62</b>	<b>2.83</b>	<b>39.61</b>	<b>356.53</b>
<b>15</b>	<b>27</b>	<b>8.34</b>	<b>4.58</b>	<b>2.79</b>	<b>40.02</b>	<b>352.50</b>
<b>20</b>	<b>20</b>	<b>8.31</b>	<b>4.44</b>	<b>2.71</b>	<b>40.44</b>	<b>339.15</b>

**Table 2: Shows the variation of dielectric properties and AC conductivity of the NiFe<sub>2</sub>O<sub>4</sub>/graphene platelets nano composite.**

<b>Graphene Content</b>	<b>Dielectric Constant at 100 Hz</b>	<b>Dielectric Loss at 100 Hz</b>	<b>Tan Loss at 100 Hz</b>	<b>AC Conductivity at 100 Hz</b>	<b>AC Impedance at 100 Hz</b>
<b>0.0</b>	<b>1.17x10<sup>4</sup></b>	<b>5.15x10<sup>3</sup></b>	<b>0.80</b>	<b>1.70x10<sup>-4</sup></b>	<b>1.36x10<sup>14</sup></b>
<b>5</b>	<b>2.51x10<sup>11</sup></b>	<b>7.57x10<sup>13</sup></b>	<b>7.97x10<sup>3</sup></b>	<b>8.69x10<sup>6</sup></b>	<b>6.07x10<sup>13</sup></b>
<b>10</b>	<b>1.00x10<sup>13</sup></b>	<b>1.15x10<sup>16</sup></b>	<b>5.70x10<sup>4</sup></b>	<b>1.23x10<sup>9</sup></b>	<b>8.61x10<sup>12</sup></b>
<b>15</b>	<b>1.76x10<sup>14</sup></b>	<b>2.22x10<sup>17</sup></b>	<b>1.54x10<sup>5</sup></b>	<b>2.46x10<sup>10</sup></b>	<b>6.75x10<sup>11</sup></b>
<b>20</b>	<b>3.82x10<sup>15</sup></b>	<b>2.96x10<sup>19</sup></b>	<b>7.31x10<sup>5</sup></b>	<b>5.30x10<sup>11</sup></b>	<b>1x10<sup>10</sup></b>

## References:

- [1] D.S. Mathew, R.-S. Juang, An overview of the structure and magnetism of spinel ferrite nanoparticles and their synthesis in microemulsions, *Chemical Engineering Journal*, 129 (2007) 51-65.
- [2] O. ur Rahman, S.C. Mohapatra, S. Ahmad, Fe<sub>3</sub>O<sub>4</sub> inverse spinel super paramagnetic nanoparticles, *Materials Chemistry and Physics*, 132 (2012) 196-202.
- [3] C. Heck, *Magnetic materials and their applications*, Elsevier, 2013.
- [4] C. Ederer, N.A. Spaldin, Weak ferromagnetism and magnetoelectric coupling in bismuth ferrite, *Physical Review B*, 71 (2005) 060401.
- [5] S. Bedanta, W. Kleemann, Supermagnetism, *Journal of Physics D: Applied Physics*, 42 (2008) 013001.
- [6] R.A. Flinn, P.K. Trojan, *Engineering materials and their applications, Engineering Materials and Their Applications*, 4th Edition, by Richard A. Flinn, Paul K. Trojan, pp. 1056. ISBN 0-471-12508-3. Wiley-VCH, December 1994., (1994) 1056.
- [7] F. Morin, Oxides which show a metal-to-insulator transition at the Neel temperature, *Physical Review Letters*, 3 (1959) 34.
- [8] X. Hong, Y. Xie, X. Wang, M. Li, Z. Le, Y. Gao, Y. Huang, Y. Qin, Y. Ling, A novel ternary hybrid electromagnetic wave-absorbing composite based on BaFe<sub>11.92</sub>(LaNd)<sub>0.04</sub>O<sub>19</sub>-titanium dioxide/multiwalled carbon nanotubes/polythiophene, *Composites Science and Technology*, 117 (2015) 215-224.
- [9] J. Li, F. Chen, Z. Liu, X. Zhao, K. Yang, W. Lu, K. Cui, Bottom-up versus top-down effects on ciliate community composition in four eutrophic lakes (China), *European journal of protistology*, 53 (2016) 20-30.
- [10] I. Gul, W. Ahmed, A. Maqsood, Electrical and magnetic characterization of nanocrystalline Ni-Zn ferrite synthesis by co-precipitation route, *Journal of Magnetism and Magnetic Materials*, 320 (2008) 270-275.
- [11] M. Gabal, Y. Al Angari, Effect of chromium ion substitution on the electromagnetic properties of nickel ferrite, *Materials Chemistry and Physics*, 118 (2009) 153-160.
- [12] R. Valenzuela, Novel applications of ferrites, *Physics Research International*, 2012 (2012).
- [13] Y. Lei, J. Li, Y. Wang, L. Gu, Y. Chang, H. Yuan, D. Xiao, Rapid microwave-assisted green synthesis of 3D hierarchical flower-shaped NiCo<sub>2</sub>O<sub>4</sub> microsphere for high-performance supercapacitor, *ACS applied materials & interfaces*, 6 (2014) 1773-1780.
- [14] Y. Yang, H. Fei, G. Ruan, C. Xiang, J.M. Tour, Efficient electrocatalytic oxygen evolution on amorphous nickel-cobalt binary oxide nanoporous layers, *ACS nano*, 8 (2014) 9518-9523.
- [15] F. Zheng, D. Zhu, Q. Chen, Facile Fabrication of Porous Ni<sub>x</sub>Co<sub>3-x</sub>O<sub>4</sub> Nanosheets with Enhanced Electrochemical Performance As Anode Materials for Li-Ion Batteries, *ACS applied materials & interfaces*, 6 (2014) 9256-9264.
- [16] Z. Yin, Q. Zheng, S.-C. Chen, D. Cai, Interface control of semiconducting metal oxide layers for efficient and stable inverted polymer solar cells with open-circuit voltages over 1.0 volt, *ACS applied materials & interfaces*, 5 (2013) 9015-9025.
- [17] V. Augustyn, P. Simon, B. Dunn, Pseudocapacitive oxide materials for high-rate electrochemical energy storage, *Energy & Environmental Science*, 7 (2014) 1597-1614.

- [18] H. Zhang, S. Gao, N. Shang, C. Wang, Z. Wang, Copper ferrite–graphene hybrid: a highly efficient magnetic catalyst for chemoselective reduction of nitroarenes, *RSC Advances*, 4 (2014) 31328-31332.
- [19] Y. Fu, Q. Chen, M. He, Y. Wan, X. Sun, H. Xia, X. Wang, Copper ferrite-graphene hybrid: a multifunctional heteroarchitecture for photocatalysis and energy storage, *Industrial & Engineering Chemistry Research*, 51 (2012) 11700-11709.
- [20] A. Ambrosi, C.K. Chua, A. Bonanni, M. Pumera, Electrochemistry of graphene and related materials, *Chemical reviews*, 114 (2014) 7150-7188.
- [21] J. Chen, C. Li, G. Shi, Graphene materials for electrochemical capacitors, *The journal of physical chemistry letters*, 4 (2013) 1244-1253.
- [22] D. Chen, H. Feng, J. Li, Graphene oxide: preparation, functionalization, and electrochemical applications, *Chemical reviews*, 112 (2012) 6027-6053.
- [23] Y. Huang, J. Liang, Y. Chen, An overview of the applications of graphene- based materials in supercapacitors, *Small*, 8 (2012) 1805-1834.
- [24] X. Zhang, X. Sun, Y. Chen, D. Zhang, Y. Ma, One-step solvothermal synthesis of graphene/Mn<sub>3</sub>O<sub>4</sub> nanocomposites and their electrochemical properties for supercapacitors, *Materials Letters*, 68 (2012) 336-339.
- [25] B. Jang, O.B. Chae, S.-K. Park, J. Ha, S.M. Oh, H.B. Na, Y. Piao, Solventless synthesis of an iron-oxide/graphene nanocomposite and its application as an anode in high-rate Li-ion batteries, *Journal of Materials Chemistry A*, 1 (2013) 15442-15446.
- [26] M.J. Allen, V.C. Tung, R.B. Kaner, Honeycomb carbon: a review of graphene, *Chemical reviews*, 110 (2009) 132-145.
- [27] X. Huang, C. Tan, Z. Yin, H. Zhang, 25th Anniversary Article: Hybrid Nanostructures Based on Two- Dimensional Nanomaterials, *Advanced Materials*, 26 (2014) 2185-2204.
- [28] M. Kurtinaitiene, K. Mazeika, S. Ramanavicius, V. Pakstas, A. Jagminas, Effect of additives on the hydrothermal synthesis of manganese ferrite nanoparticles, *Advances in nano research*, 4 (2016) 1-14.
- [29] B. Ong, E. Chee, S. Abd Hamid, K. Lim, K. Noorsal, A. Masrom, Synthesis and characterization of nickel ferrite magnetic nanoparticles by co-precipitation method, in: *AIP Conference Proceedings*, AIP, 2012, pp. 221-229.
- [30] I. Gul, A. Maqsood, Structural, magnetic and electrical properties of cobalt ferrites prepared by the sol–gel route, *Journal of Alloys and Compounds*, 465 (2008) 227-231.
- [31] Y. Tang, X. Wang, Q. Zhang, Y. Li, H. Wang, Solvothermal synthesis of Co<sub>1-x</sub>Ni<sub>x</sub>Fe<sub>2</sub>O<sub>4</sub> nanoparticles and its application in ammonia vapors detection, *Progress in Natural Science: Materials International*, 22 (2012) 53-58.
- [32] K. Pemartin, C. Solans, J. Alvarez-Quintana, M. Sanchez-Dominguez, Synthesis of Mn–Zn ferrite nanoparticles by the oil-in-water microemulsion reaction method, *Colloids and Surfaces A: Physicochemical and Engineering Aspects*, 451 (2014) 161-171.
- [33] E.L. Crepaldi, P.C. Pavan, J.B. Valim, Comparative study of the coprecipitation methods for the preparation of layered double hydroxides, *Journal of the Brazilian Chemical Society*, 11 (2000) 64-70.
- [34] J. Allen Matthew, C. Tung Vincent, B. Kaner Richard, Honeycomb carbon a review of graphene, *Chem. Rev*, 110 (2010) 132-145.

- [35] A.A. Ali, M. Eltabey, B.M. Abdelbary, S.H. Zoalfakar, MWCNTs/carbon nano fibril composite papers for fuel cell and super capacitor applications, *Journal of Electrostatics*, 73 (2015) 12-18.
- [36] O.A. Al-Hartomy, A.A. Al-Ghamdi, F. Al-Salamy, N. Dishovsky, R. Shtarkova, V. Iliev, F. El-Tantawy, Dielectric and microwave properties of graphene nanoplatelets/carbon black filled natural rubber composites, *International Journal of Materials and Chemistry*, 2 (2012) 116-122.
- [37] A. Paladino, J. Waugh, J. Green, A. Booth, Fine- Grain Nickel Ferrite for Microwave Applications at High Peak- Power Levels, *Journal of Applied Physics*, 37 (1966) 3371-3377.
- [38] M. LEVIN, M. MILLER, Maxwell a treatise on electricity and magnetism, *Uspekhi Fizicheskikh Nauk*, 135 (1981) 425-440.
- [39] R.S. Alam, M. Moradi, H. Nikmanesh, Influence of multi-walled carbon nanotubes (MWCNTs) volume percentage on the magnetic and microwave absorbing properties of BaMg 0.5 Co 0.5 TiFe 10 O 19/MWCNTs nanocomposites, *Materials Research Bulletin*, 73 (2016) 261-267.
- [40] Z. Durmus, A. Durmus, H. Kavas, Synthesis and characterization of structural and magnetic properties of graphene/hard ferrite nanocomposites as microwave-absorbing material, *Journal of Materials Science*, 50 (2015) 1201-1213.
- [41] Z. Wang, J. Luo, G.L. Zhao, Dielectric and microwave attenuation properties of graphene nanoplatelet–epoxy composites, *AIP Advances*, 4 (2014) 017139.
- [42] S. Ameer, I.H. Gul, Influence of Reduced Graphene Oxide on Effective Absorption Bandwidth Shift of Hybrid Absorbers, *PloS one*, 11 (2016) e0153544.
- [43] L. Zhang, X. Yu, H. Hu, Y. Li, M. Wu, Z. Wang, G. Li, Z. Sun, C. Chen, Facile synthesis of iron oxides/reduced graphene oxide composites: application for electromagnetic wave absorption at high temperature, *Scientific reports*, 5 (2015) 9298.
- [44] J. Ai, E. Biazar, M. Jafarpour, M. Montazeri, A. Majdi, S. Aminifard, M. Zafari, H.R. Akbari, H.G. Rad, Nanotoxicology and nanoparticle safety in biomedical designs, *Int J Nanomedicine*, 6 (2011) 1117-1127.
- [45] X. Yuan, B. Liu, H. Hou, K. Zeinu, Y. He, X. Yang, W. Xue, X. He, L. Huang, X. Zhu, Facile synthesis of mesoporous graphene platelets with in situ nitrogen and sulfur doping for lithium–sulfur batteries, *RSC Advances*, 7 (2017) 22567-22577.
- [46] D. Kumar, K. Singh, V. Verma, H. Bhatti, Microwave assisted synthesis and characterization of graphene nanoplatelets, *Applied Nanoscience*, 6 (2016) 97-103.
- [47] R. Ahmad, I.H. Gul, M. Zarrar, H. Anwar, M.B. Khan Niazi, A. Khan, Improved electrical properties of cadmium substituted cobalt ferrites nano-particles for microwave application, *Journal of Magnetism and Magnetic Materials*, 405 (2016) 28-35.
- [48] I. Gul, A. Abbasi, F. Amin, M. Anis-ur-Rehman, A. Maqsood, Structural, magnetic and electrical properties of Co 1– xZnxFe 2 O 4 synthesized by co-precipitation method, *Journal of Magnetism and Magnetic Materials*, 311 (2007) 494-499.
- [49] Y. Zhang, Z. Yang, D. Yin, Y. Liu, C. Fei, R. Xiong, J. Shi, G. Yan, Composition and magnetic properties of cobalt ferrite nano-particles prepared by the co-precipitation method, *Journal of Magnetism and Magnetic Materials*, 322 (2010) 3470-3475.
- [50] A. Trovarelli, *Catalysis by ceria and related materials*, World Scientific, 2002.
- [51] H. Xie, G. Hu, K. Du, Z. Peng, Y. Cao, An improved continuous co-precipitation method to synthesize LiNi 0.80 Co 0.15 Al 0.05 O 2 cathode material, *Journal of Alloys and Compounds*, 666 (2016) 84-87.

- [52] R. Melo, F. Silva, K. Moura, A. de Menezes, F. Sinfrônio, Magnetic ferrites synthesised using the microwave-hydrothermal method, *Journal of Magnetism and Magnetic Materials*, 381 (2015) 109-115.
- [53] H.P. Klug, L.E. Alexander, X-ray diffraction procedures, (1954).
- [54] Z.G. Özdemir, N.Y. Canli, B. Senkal, Y. Gürsel, M. Okutan, Super-capacitive behavior of carbon nano tube doped 11-(4-cyanobiphenyl-4-oxy) undecan-1-ol, *Journal of Molecular Liquids*, 211 (2015) 442-447.
- [55] N.J. Unakar, J.Y. Tsui, C.V. Harding, Scanning electron microscopy, *Ophthalmic Research*, 13 (1981) 20-35.
- [56] G. Nabiyouni, M.J. Fesharaki, M. Mozafari, J. Amighian, Characterization and magnetic properties of nickel ferrite nanoparticles prepared by ball milling technique, *Chinese Physics Letters*, 27 (2010) 126401.
- [57] S.J. Jayaseelan, K. Parasuraman, M. Anbarasu, K. Balamurugan, Synthesis and Characterization of NiFe<sub>2</sub>O<sub>4</sub> Nanoparticles by Chemical Co-precipitation Method.
- [58] J. Tate, H. Ju, J. Moon, A. Zakutayev, A. Richard, J. Russell, D. McIntyre, Origin of p-type conduction in single-crystal CuAlO<sub>2</sub>, *Physical review B*, 80 (2009) 165206.
- [59] K.W. Wagner, Zur theorie der unvollkommenen dielektrika, *Annalen der Physik*, 345 (1913) 817-855.
- [60] C. Koops, On the dispersion of resistivity and dielectric constant of some semiconductors at audiofrequencies, *Physical Review*, 83 (1951) 121.
- [61] R. Samkaria, V. Sharma, Structural, dielectric and electrical studies of MgAl<sub>2-2x</sub>Y<sub>2x</sub>O<sub>4</sub> (x= 0.00–0.05) cubic spinel nano aluminate, *Journal of Electroceramics*, 31 (2013) 67-74.
- [62] K. Wagner, The theory of incomplete dielectricity, *Ann. Phys*, 40 (1913) 817.
- [63] I. Gul, A. Maqsood, M. Naeem, M.N. Ashiq, Optical, magnetic and electrical investigation of cobalt ferrite nanoparticles synthesized by co-precipitation route, *Journal of alloys and compounds*, 507 (2010) 201-206.
- [64] I. Austin, N.F. Mott, Polarons in crystalline and non-crystalline materials, *Advances in Physics*, 18 (1969) 41-102.
- [65] K.S. Cole, R.H. Cole, Dispersion and absorption in dielectrics II. Direct current characteristics, *The Journal of Chemical Physics*, 10 (1942) 98-105.
- [66] J. Liu, C.-g. Duan, W.-N. Mei, R.W. Smith, J.R. Hardy, Dielectric properties and Maxwell-Wagner relaxation of compounds A Cu<sub>3</sub> Ti<sub>4</sub> O<sub>12</sub> (A= Ca, Bi<sup>2/3</sup>, Y<sup>2/3</sup>, La<sup>2/3</sup>), *Journal of applied Physics*, 98 (2005) 093703.
- [67] R. Laishram, S. Phanjoubam, H. Sarma, C. Prakash, Electrical and magnetic studies of the spinel system Li<sub>0.5+t</sub> Cr<sub>x</sub>Sb<sub>t</sub> Fe<sub>2.5-x-2t</sub>O<sub>4</sub>, *Journal of Physics D: Applied Physics*, 32 (1999) 2151.
- [68] L. Harris, Preparation and infrared properties of aluminum oxide films, *JOSA*, 45 (1955) 27-29.
- [69] M. Amer, T. Meaz, A. Mostafa, M. El-Kastawi, A. Ghoneim, Characterization and spectral studies of Co<sup>3+</sup>-doped Cd<sub>0.4</sub> Mn<sub>0.6</sub> Fe<sub>2</sub> O<sub>4</sub> ferrites, *Ceramics International*, 40 (2014) 241-248.
- [70] M. Rashad, A. Shalan, M. Lira-Cantu, M. Abdel-Mottaleb, Synthesis and characterization of mesoporous anatase TiO<sub>2</sub> nanostructures via organic acid precursor process for dye-sensitized solar cells applications, *Journal of Industrial and Engineering Chemistry*, 19 (2013) 2052-2059.

## Conclusion:

The NiFe<sub>2</sub>O<sub>4</sub> nano particles were successfully prepared using wet chemical co-precipitation method. The nano composite of NiFe<sub>2</sub>O<sub>4</sub>/graphene platelets was successfully synthesized in varying percentage of graphene (x= 0.0%, 5%, 10%, 15%, 20%) using dispersion method. Water was successfully used as a dispersive medium for dispersion of graphene platelets and nickel ferrite nano particles. X-ray diffraction (XRD) studies reveal the formation of face centered cubic phase. The crystallite size was calculated using Scherer formula and was obtained to be in the range of 20nm to 30nm. The decrease in crystallite size is due to incorporation of graphene platelets in nickel ferrite that will cause reduction of grain size. There was no other peak present indicating purity of material. The decrease in bulk and x-ray density is due to presence of porous structure of graphene platelets. The porous nature of graphene platelets also resulted in increased porosity. The successful attachment of NiFe<sub>2</sub>O<sub>4</sub> nano particles on graphene plates were observed using scanning electron microscopy (SEM). The size of particles obtained from scanning electron microscopy is in agreement with size calculated using Scherer formula. The fourier transform infrared spectroscopy (FTIR) spectra show the bands in the range of (339 cm<sup>-1</sup> to 400 cm<sup>-1</sup>) for octahedral sites and (579 cm<sup>-1</sup> to 600 cm<sup>-1</sup>) for tetrahedral sites. The dielectric properties of NiFe<sub>2</sub>O<sub>4</sub>/graphene platelets showed a huge enhancement leading towards super capacitor behavior of prepared nano composite. The increase in the properties can be attributed to the high surface area and conductive nature of graphene platelets. The values of dielectric loss has also increased. Therefore low graphene platelets content is needed in cases where minimum dielectric loss is required. The AC conductivity trends shows that the conductive nature of graphene platelets assist hopping mechanism resulting in increased AC conductivity. The experimental route proved to be an efficient, inexpensive and straight forward procedure for the synthesis of ferrite/graphene platelets nano composite.



## **Future work:**

The optical properties of prepared nano composites can be studied using UV-Visible spectroscopy and can be applicable in many applications including military applications.

The composite with different polymers can be made in order to study different properties including mechanical, electrical and optical properties.

The polymerization can be used for preparing different compositions of polymer blends. The effect of mechanical, dielectric and microwave properties can also be studied by making its composite with desired polymer.

These nano composite show remarkable dielectric properties so they can be applicable in cathode of batteries, super capacitors or resins. These applications involve large strength and stiffness even at elevated temperatures.

The prepared nano composite can render very useful in various industrial applications. Such a versatile nano composite can make remarkable nuisance in fields of dielectric, microwave, electromagnetic, optical and magnetic applications.